

University of Montana

## ScholarWorks at University of Montana

---

Chemistry and Biochemistry Faculty  
Publications

Chemistry and Biochemistry

---

8-12-2015

# Biomass burning emissions and potential air quality impacts of volatile organic compounds and other trace gases from temperate fuels common in the United States

J. B. Gilman

*University of Colorado Boulder*

B. M. Lerner

*University of Colorado Boulder*

W. C. Kuster

*University of Colorado Boulder*

P. D. Goldan

*University of Colorado Boulder*

C. Warneke

*University of Colorado Boulder*

Follow this and additional works at: [https://scholarworks.umt.edu/chem\\_pubs](https://scholarworks.umt.edu/chem_pubs)

See next page for additional authors

 Part of the [Biochemistry Commons](#), and the [Chemistry Commons](#)

## Let us know how access to this document benefits you.

---

### Recommended Citation

Gilman, J. B.; Lerner, B. M.; Kuster, W. C.; Goldan, P. D.; Warneke, C.; Veres, P. R.; Roberts, J. M.; de Gouw, J. A.; Burling, I. R.; and Yokelson, Robert, "Biomass burning emissions and potential air quality impacts of volatile organic compounds and other trace gases from temperate fuels common in the United States" (2015). *Chemistry and Biochemistry Faculty Publications*. 89.  
[https://scholarworks.umt.edu/chem\\_pubs/89](https://scholarworks.umt.edu/chem_pubs/89)

This Article is brought to you for free and open access by the Chemistry and Biochemistry at ScholarWorks at University of Montana. It has been accepted for inclusion in Chemistry and Biochemistry Faculty Publications by an authorized administrator of ScholarWorks at University of Montana. For more information, please contact [scholarworks@mso.umt.edu](mailto:scholarworks@mso.umt.edu).

---

**Authors**

J. B. Gilman, B. M. Lerner, W. C. Kuster, P. D. Goldan, C. Warneke, P. R. Veres, J. M. Roberts, J. A. de Gouw, I. R. Burling, and Robert Yokelson



This discussion paper is/has been under review for the journal Atmospheric Chemistry and Physics (ACP). Please refer to the corresponding final paper in ACP if available.

# Biomass burning emissions and potential air quality impacts of volatile organic compounds and other trace gases from temperate fuels common in the United States

J. B. Gilman<sup>1,2</sup>, B. M. Lerner<sup>1,2</sup>, W. C. Kuster<sup>1,2,a</sup>, P. D. Goldan<sup>1,2,a</sup>, C. Warneke<sup>1,2</sup>, P. R. Veres<sup>1,2</sup>, J. M. Roberts<sup>2</sup>, J. A. de Gouw<sup>1,2</sup>, I. R. Burling<sup>3,b</sup>, and R. J. Yokelson<sup>3</sup>

<sup>1</sup>CIRES at University of Colorado, Boulder, CO, USA

<sup>2</sup>NOAA Earth System Research Laboratory, Boulder, CO, USA

<sup>3</sup>Department of Chemistry, University of Montana, Missoula, Montana, USA

<sup>a</sup>now retired

<sup>b</sup>now at: Cytec Canada, Niagara Falls, Ontario, Canada

## Biomass burning emissions and potential air quality impacts

J. B. Gilman et al.

Title Page

Abstract

Introduction

Conclusions

References

Tables

Figures



Back

Close

Full Screen / Esc

Printer-friendly Version

Interactive Discussion



Received: 2 July 2015 – Accepted: 28 July 2015 – Published: 12 August 2015

Correspondence to: J. B. Gilman (jessica.gilman@noaa.gov)

Published by Copernicus Publications on behalf of the European Geosciences Union.

**ACPD**

15, 21713–21763, 2015

**Biomass burning  
emissions and  
potential air quality  
impacts**

J. B. Gilman et al.

Title Page

Abstract

Introduction

Conclusions

References

Tables

Figures



Back

Close

Full Screen / Esc

Printer-friendly Version

Interactive Discussion



## Abstract

A comprehensive suite of instruments was used to quantify the emissions of over 200 organic gases, including methane and volatile organic compounds (VOCs), and 9 inorganic gases from 56 laboratory burns of 18 different biomass fuel types common in the southeastern, southwestern, or northern United States. A gas chromatograph-mass spectrometer (GC-MS) provided extensive chemical detail of discrete air samples collected during a laboratory burn and was complemented by real-time measurements of organic and inorganic species via an open-path Fourier transform infrared spectrometer (OP-FTIR) and 3 different chemical ionization-mass spectrometers. These measurements were conducted in February 2009 at the U.S. Department of Agriculture's Fire Sciences Laboratory in Missoula, Montana. The relative magnitude and composition of the gases emitted varied by individual fuel type and, more broadly, by the 3 geographic fuel regions being simulated. Emission ratios relative to carbon monoxide (CO) were used to characterize the composition of gases emitted by mass; reactivity with the hydroxyl radical, OH; and potential secondary organic aerosol (SOA) precursors for the 3 different US fuel regions presented here. VOCs contributed less than  $0.78 \pm 0.12\%$  of emissions by mole and less than  $0.95 \pm 0.07\%$  of emissions by mass (on average) due to the predominance of  $\text{CO}_2$ , CO,  $\text{CH}_4$ , and  $\text{NO}_x$  emissions; however, VOCs contributed 70–90 ( $\pm 16$ )% to OH reactivity and were the only measured gas-phase source of SOA precursors from combustion of biomass. Over 82% of the VOC emissions by mole were unsaturated compounds including highly reactive alkenes and aromatics and photolabile oxygenated VOCs (OVOCs) such as formaldehyde. OVOCs contributed 57–68% of the VOC mass emitted, 42–57% of VOC-OH reactivity, and aromatic-OVOCs such as benzenediols, phenols, and benzaldehyde were the dominant potential SOA precursors. In addition, ambient air measurements of emissions from the Fourmile Canyon Fire that affected Boulder, Colorado in September 2010 allowed us to investigate biomass burning (BB) emissions in the presence of other VOC

### Biomass burning emissions and potential air quality impacts

J. B. Gilman et al.

Title Page

Abstract

Introduction

Conclusions

References

Tables

Figures



Back

Close

Full Screen / Esc

Printer-friendly Version

Interactive Discussion



sources (i.e., urban and biogenic emissions) and identify several promising BB markers including benzofuran, 2-furaldehyde, 2-methylfuran, furan, and benzonitrile.

## 1 Introduction

Biomass burning (BB) emissions are composed of a complex mixture of gases and particles that may directly and/or indirectly affect both climate and air quality (Jaffe and Wigder, 2012; Sommers et al., 2014). Emissions include greenhouse gases such as carbon dioxide (CO<sub>2</sub>), methane (CH<sub>4</sub>), and nitrous oxide (N<sub>2</sub>O); carcinogens such as formaldehyde and benzene; and other components harmful to human health including particulate matter, carbon monoxide (CO) and isocyanic acid (HNCO) (Crutzen and Andreae, 1990; Hegg et al., 1990; Andreae and Merlet, 2001; Demirbas and Demirbas, 2009; Estrellan and Iino, 2010; Roberts et al., 2010, 2011; Sommers et al., 2014). The co-emission of nitrogen oxides (NO<sub>x</sub> = NO + NO<sub>2</sub>) and reactive volatile organic compounds (VOCs, also known as non-methane organic compounds) from combustion of biomass may degrade local and regional air quality by the photochemical formation of tropospheric ozone (O<sub>3</sub>), a hazardous air pollutant, and secondary organic aerosol (SOA) (Alvarado et al., 2015). This work is aimed at characterizing primary biomass burning emissions of organic and inorganic gases in order to identify key species that may contribute to O<sub>3</sub> and/or SOA formation.

Tropospheric O<sub>3</sub> may be formed in the atmosphere from the interactions of VOCs, NO<sub>x</sub>, and a radical source such as the hydroxyl radical (OH), which is formed from the photolysis of O<sub>3</sub>, aldehydes, hydroperoxides, or nitrous acid (HONO). OH is a key oxidant in the troposphere and it plays a pivotal role in determining the atmospheric lifetimes of reactive organic and inorganic gases. Oxidation of VOCs and other gases such as CO and CH<sub>4</sub> by OH leads to the formation of alkyl (R•), alkoxy (RO•), and alkylperoxy (RO<sub>2</sub>•) radicals, where R represents a carbon-containing derivative. These radicals are important, but short-lived, intermediaries that aid in the conversion of NO to NO<sub>2</sub>. Photolysis of NO<sub>2</sub> produced from the reaction of RO<sub>2</sub>• + NO is the principal

### Biomass burning emissions and potential air quality impacts

J. B. Gilman et al.

Title Page

Abstract

Introduction

Conclusions

References

Tables

Figures



Back

Close

Full Screen / Esc

Printer-friendly Version

Interactive Discussion



**Biomass burning emissions and potential air quality impacts**

J. B. Gilman et al.

Title Page

Abstract

Introduction

Conclusions

References

Tables

Figures

◀

▶

◀

▶

Back

Close

Full Screen / Esc

Printer-friendly Version

Interactive Discussion



source of tropospheric O<sub>3</sub>; however, the amount of O<sub>3</sub> formed is dependent on the relative abundances of NO<sub>x</sub> and VOCs (Carter, 1994). Biomass burning is a large, primary source of VOCs, NO<sub>x</sub>, and HONO (i.e., O<sub>3</sub> precursors); however, these species are emitted at varying relative ratios depending on the fuel type and burn conditions making it difficult to predict O<sub>3</sub> formation from the combustion of biomass (Akagi et al., 2011; Jaffe and Wigder, 2012). An additional O<sub>3</sub> formation pathway involves the formation of peroxy nitrates, such as peroxyacetic nitric anhydride (PAN), via R(O)O<sub>2</sub>• + NO<sub>2</sub> reaction. This pathway may diminish O<sub>3</sub> formation in fresh BB plumes due to the initial sequestration of NO<sub>2</sub>, but enhance O<sub>3</sub> downwind formation via production of NO<sub>2</sub> from thermal dissociation of peroxy nitrates (Jaffe and Wigder, 2012).

SOA is organic particulate mass that is formed in the atmosphere from the chemical evolution of primary emissions of organic species. Here, chemical evolution refers to a complex series of reactions of a large number of organic species that results in the formation of relatively low volatility and/or high solubility oxidation products that will readily partition to, or remain in, the particle phase (Kroll and Seinfeld, 2008). Oxidation may occur via addition of OH, O<sub>3</sub>, or the nitrate radical (NO<sub>3</sub>) to a double bond or result from the reactions of the RO<sub>2</sub>• and/or RO• radicals formed from hydrogen abstraction of the parent compound. These pathways may result in oxidation products that contain polar functional groups such as ketones, aldehydes, alcohols, nitrates, and carboxylic acids that can have vapor pressures approximately 10 to 10 000 times lower than their parent compounds (Pankow, 1994) allowing for more efficient partitioning to the particulate phase. Thus, VOCs that are considered to be efficient SOA precursors are relatively reactive organic compounds whose oxidation products are of sufficiently low volatility and/or higher solubility than the parent VOC. SOA formation from BB emissions is highly variable and chemical modeling results suggest that there is a “missing large source of SOA” precursors that cannot be explained by known SOA precursors such as toluene (Alvarado et al., 2015).

Advances in instrumentation and complementary measurement approaches have enabled chemical analyses of a wide range of species emitted during laboratory-based







**Biomass burning emissions and potential air quality impacts**

J. B. Gilman et al.

Title Page

Abstract

Introduction

Conclusions

References

Tables

Figures



Back

Close

Full Screen / Esc

Printer-friendly Version

Interactive Discussion



9 southwestern fuels from southern California and Arizona including chaparral shrub, mesquite, and oak savanna/woodland; 6 southeastern fuels represented the pine savanna/shrub complexes indigenous to coastal North Carolina and pine litter from Georgia; and 3 northern fuels including an Englemann spruce, a grand fir, and ponderosa pine needles from Montana. All fuels were harvested in January 2009 and sent to the Fire Sciences Laboratory where they were stored in a walk-in cooler prior to these experiments.

All biomass burns were conducted inside the large burn chamber (12.5 m × 12.5 m × 20 m height), which contains a fuel bed under an emissions-entraining hood, an exhaust stack, and an elevated sampling platform surrounding the exhaust stack approximately 17 m above the fuel bed (Christian et al., 2003, 2004; Burling et al., 2010). Each fuel sample was arranged on the fuel bed in a manner that mimicked their natural orientation and fuel loading when possible and was ignited using a small propane torch (Burling et al., 2010). During each fire, the burn chamber was slightly pressurized with outside air conditioned to a similar temperature and relative humidity as the ambient air inside the burn chamber. The subsequent emissions were entrained by the pre-conditioned ambient air and continuously vented through the top of the exhaust stack. The residence time of emissions in the exhaust stack ranged from ~ 5 to 17 s depending on the flow/vent rate. Each burn lasted approximately 20–40 min from ignition to natural extinction.

## 2.2 Instrumentation and sampling

A list of the gas-phase instruments used in this study, a brief description of their inherent sampling limitations, and references appears in Table 1. The gas chromatograph mass spectrometer (GC-MS) and the proton-transfer-reaction mass spectrometer (PTR-MS) were located in a laboratory adjacent to the burn chamber. The proton-transfer-reaction ion-trap mass spectrometer (PIT-MS), negative-ion proton-transfer chemical-ionization mass spectrometer (NI-PT-CIMS), and open-path Fourier trans-





**Biomass burning emissions and potential air quality impacts**

J. B. Gilman et al.

Title Page

Abstract

Introduction

Conclusions

References

Tables

Figures



Back

Close

Full Screen / Esc

Printer-friendly Version

Interactive Discussion



C<sub>4</sub>H<sub>4</sub>), methyl nitrite (CH<sub>3</sub>ONO), nitromethane (CH<sub>3</sub>NO<sub>2</sub>), methyl pyrazole (C<sub>4</sub>H<sub>6</sub>N<sub>2</sub>), ethyl pyrazine (C<sub>6</sub>H<sub>8</sub>N<sub>2</sub>), and tricarbon dioxide (carbon suboxide, C<sub>3</sub>O<sub>2</sub>). For some species, we were able to identify the chemical family (defined by its molecular formula and common chemical moiety) but not the exact chemical structure or identity. For these cases, we present the emissions as a sum of the unidentified isomers for a particular chemical family (see Table 2). We report only the compounds that were above the limits of detection for the majority of the biomass burns and where the molecular formula could be identified.

Of the 187 gases quantified by the GC-MS in this study, 95 were individually calibrated with commercially available and/or custom-made gravimetrically-based compressed gas calibration standards. The limit of detection, precision, and accuracy are compound dependent, but are conservatively better than 0.010 ppbv, 15, and 25%, respectively (Gilman et al., 2009, 2010). For compounds where a calibration standard was not available, the calibration factors were estimated using measured calibrations of compounds in a similar chemical family with a similar retention time, and when possible a similar mass fragmentation pattern. In order to estimate the uncertainty in the accuracy of un-calibrated species, we use measured calibrations of ethyl benzene, o-xylene, and the sum of m- and p-xylenes as a test case. These aromatic species have similar mass fragmentation patterns, are all quantified using *m/z* 91, and elute within 1 min of each other signifying similar physical properties. If a single calibration factor was used for all these isomers, then the reported mixing ratios could be miscalculated by up to 34%. We therefore conservatively estimate the accuracy of all un-calibrated species as 50%.

## 2.4 Calculation of emission ratios

Emission ratios (ER) to carbon monoxide (CO) for each gas-phase compound,  $X$ , were calculated as follows:

$$ER = \frac{\Delta X}{\Delta CO} = \frac{\int_{t_{\text{start}}}^{t_{\text{end}}} (X_{\text{fire}} - X_{\text{bknd}}) dt}{\int_{t_{\text{start}}}^{t_{\text{end}}} (CO_{\text{fire}} - CO_{\text{bknd}}) dt} \quad (1)$$

where  $\Delta X$  and  $\Delta CO$  are the excess mixing ratios of compound  $X$  or CO, respectively, during a fire above the background. Background values,  $X_{\text{bknd}}$  and  $CO_{\text{bknd}}$ , are equal to the average mixing ratio of a species in the pre-conditioned ambient air inside the exhaust stack in the absence of a fire. For the OP-FTIR, PTR-MS, PIT-MS and NI-PT-CIMS, backgrounds were determined from the mean responses of the ambient air inside the exhaust stack for a minimum of 60 s prior to the ignition of each fire. At least one background sample was collected for the GC-MS each day. The composition and average mixing ratios of VOCs in the stack backgrounds were consistent over the course of the campaign and were generally much lower than the mixing ratios observed during biomass burns. For example, the average background ethyne measured by the GC-MS was  $1.22 \pm 0.33$  ppbv (median = 1.21 ppbv) compared to a mean ethyne of  $150 \pm 460$  ppbv (median = 42 ppbv) in the fires. The large standard deviation for ethyne in the biomass burns reflects the large variability in ethyne emissions rather than uncertainty in the measurement.

The type of emission ratio, discrete or fire-integrated, is determined by the sampling frequency of the instrument and sampling duration. The GC-MS is only capable of measuring discrete ERs, which represent the average  $\Delta X$  relative to  $\Delta CO$  for a relatively short portion of a fire corresponding to the GC-MS sample acquisition time. The OP-FTIR, PTR-MS, and NI-PT-CIMS are fast-response instruments that sampled every 1 to 10 s over the entire duration of each fire. These measurements were used to calculate both fire-integrated ERs that represent to  $\Delta X/\Delta CO$  over the entirety of a fire ( $dt \geq 1000$  s) (Burling et al., 2010; Veres et al., 2010; Warneke et al., 2011) as well

### Biomass burning emissions and potential air quality impacts

J. B. Gilman et al.

Title Page

Abstract

Introduction

Conclusions

References

Tables

Figures



Back

Close

Full Screen / Esc

Printer-friendly Version

Interactive Discussion



as discrete ERs coincident with the GC-MS sample acquisition ( $dt = 20$  to  $300$  s) as discussed in Sect. 2.3. We reference all ERs to CO because the majority of VOCs and CO are co-emitted by smoldering combustion during the fire whereas  $\text{CO}_2$  emissions occur mostly from flaming (see Sect. 3.1). Additionally, ratios to CO are commonly reported in the literature for biomass burning and urban VOC emission sources. All data presented here are in units of ppbv VOC per ppmv CO, which is equivalent to a molar ratio ( $\text{mmol VOC}(\text{mol CO})^{-1}$ ).

## 2.5 Fourmile Canyon Fire in Boulder, Colorado

Ambient air measurements of biomass burning emissions from the Fourmile Canyon Fire that occurred in the foothills 10 km west of Boulder, Colorado were conducted from 7–9 September 2010. Over the course of the Fourmile Fire, approximately  $25 \text{ km}^2$  of land including 168 structures burned. The burned vegetation consisted primarily of Douglas-fir (*Pseudotsuga menziesii*) and ponderosa pine (*Pinus ponderosa*) mixed with juniper (*Juniperus scopulorum* and *communis*), mountain mahogany (*Cercocarpus*), and various shrubs and grasses common to the mountain zone of the Colorado Front Range (Graham et al., 2012). During the measurement period, down-sloping winds ranging from  $1$  to  $12 \text{ m s}^{-1}$  (mean =  $3.5 \text{ m s}^{-1}$ ) periodically brought biomass burning emissions to NOAA's Earth Systems Research Laboratory located at the western edge of the city of Boulder. The previously described in-situ GC-MS was housed inside the laboratory and sampled outside air via a 15 m Teflon sample line (residence time  $< 2$  s) attached to an exterior port on the western side of the building. CO was measured via a co-located vacuum-UV resonance fluorescence instrument (Gerbig et al., 1999).

### Biomass burning emissions and potential air quality impacts

J. B. Gilman et al.

Title Page

Abstract

Introduction

Conclusions

References

Tables

Figures



Back

Close

Full Screen / Esc

Printer-friendly Version

Interactive Discussion





### 3 Results and discussion

#### 3.1 Calculation of emission ratios

Temporal profiles of laboratory biomass burns provide valuable insight into the combustion chemistry and processes that lead to the emissions of various species (Yokelson et al., 1996). Figure 1 shows temporal profiles of an example burn in order to illustrate (i) flaming, mixed, and smoldering combustion phases/processes and (ii) the sampling frequencies and temporal overlap of the fast-response instruments compared to the GC-MS. Upon ignition, there is an immediate and substantial increase in  $\text{CO}_2$  and  $\text{NO}_x$  ( $\text{NO} + \text{NO}_2$ ) indicative of vigorous flaming combustion. This transitions to a mixed-phase characterized by diminishing  $\text{CO}_2$  and  $\text{NO}_x$  emissions and a second increase in  $\text{CO}$ . The fire eventually evolves to a weakly-emitting, protracted period of mostly smoldering combustion (Yokelson et al., 1996; Burling et al., 2010). Figure 1 also includes the temporal profile of the modified combustion efficiency,  $\text{MCE} = \Delta\text{CO}_2 / [\Delta\text{CO} + \Delta\text{CO}_2]$ , which is a proxy for the relative amounts of flaming and smoldering combustion (Yokelson et al., 1996). During the initial flaming phase of the fire, the MCE approaches unity due to the dominance of  $\text{CO}_2$  emissions. The MCE gradually decreases during smoldering combustion when  $\text{CO}$  emissions are more prominent.

In order to compare measurements from multiple instruments, we calculated the average excess mixing ratios of a species,  $\Delta X$ , measured by the fast-response instruments over the corresponding GC-MS sample acquisition times for all 56 biomass burns. We compare the measurements using correlation plots of  $\Delta X$  for VOCs measured by the GC-MS vs. the same compound measured by the OP-FTIR or an analogous  $m/z$  measured by the PTR-MS. The slopes and correlation coefficients,  $r$ , were determined by linear orthogonal distance regression analysis and are compiled in Fig. 2a. The average slope and standard deviation of the instrument comparison is  $1.0 \pm 0.2$  and  $0.93 < r < 0.99$  signifying good overall agreement between the different

## Biomass burning emissions and potential air quality impacts

J. B. Gilman et al.

Title Page

Abstract

Introduction

Conclusions

References

Tables

Figures

◀

▶

◀

▶

Back

Close

Full Screen / Esc

Printer-friendly Version

Interactive Discussion





measurement techniques for the species investigated here. A few comparisons are discussed in more detail below.

The largest difference between the GC-MS and the OP-FTIR observations was for propene (slope = 1.36) indicating that the GC-MS response is greater than the OP-FTIR; however, a correlation coefficient of 0.99 suggests that the offset is more likely from a calibration difference that remains unresolved. The possibility of a species with the same retention time and similar fragmentation pattern as propene that is also co-emitted at a consistent ratio relative to propene seems highly unlikely, but cannot be completely ruled out. For furan, the GC-MS had a lower response than OP-FTIR (slope = 0.77) indicating that the GC-MS may be biased low for furan or that the OP-FTIR may have spectral interferences that bias the measurement high. The temporal profiles of these measurements shown in Fig. 1 suggest that there was a spectral interference with the OP-FTIR measurement of furan as evidenced by the large emissions in the flaming phase that was not captured by the  $m/z$  69 response of the PTR-MS. These early “spurious” OP-FTIR furan responses would (i) only affect the comparison for the GC-MS samples collected in the flaming phase of the fires and (ii) have not been observed in other biomass burning experiments utilizing this OP-FTIR (Christian et al., 2004; Stockwell et al., 2014).

Comparison of the GC-MS  $\Sigma$  (isoprene + furan) vs. PTR-MS  $m/z$  69 has the lowest slope (GC-MS vs. PTR-MS = 0.64) indicating the contribution of other VOCs, e.g. cis- and trans-1,3-pentadienes, to the  $m/z$  69 response of the PTR-MS in fresh smoke (Warneke et al., 2011). Carbon suboxide ( $C_3O_2$ ) has also been shown to contribute to  $m/z$  69 response for the PTR-MS technique (Stockwell et al., 2015). Direct comparisons of the real-time measurements for a variety of other species not measured by the GC-MS (e.g., formaldehyde, formic acid, and HONO) can be found elsewhere (Burling et al., 2010; Veres et al., 2010; Warneke et al., 2011).

**Biomass burning emissions and potential air quality impacts**

J. B. Gilman et al.

Title Page

Abstract

Introduction

Conclusions

References

Tables

Figures



Back

Close

Full Screen / Esc

Printer-friendly Version

Interactive Discussion



### 3.2 Comparison of discrete and fire-integrated ERs

Fire-integrated ERs represent emissions from all combustion processes of a biomass burn whereas discrete ERs capture a relatively brief snapshot of emissions from mixed combustion processes during a particular sampling period. Figure 1 includes time series of VOC to CO ERs measured by the real-time measurement techniques for select gases. Here we compare the 2 different measurement strategies, discrete vs. fire-integrated, in order to (i) determine if the discrete ERs measured by the GC-MS may be biased by the sample acquisition times which typically occurred within the first-half of a laboratory burn when emissions for most gases generally “peaked” and (ii) assess how well the discrete GC-MS samples are able to capture the fire-to-fire variability of emissions relative to CO. We do this by determining discrete ERs for the OP-FTIR or PTR-MS for each of the 56 biomass burns using Eq. (1) where  $t_{\text{start}}$  and  $t_{\text{end}}$  times correspond to the GC-MS sample acquisition. The discrete ERs are then compared to the fire-integrated ERs measured by the same fast-response instrument so that potential measurement artifacts will not affect the comparison.

The slopes and correlation coefficients,  $r$ , of discrete vs. fire-integrated ERs for select VOCs are summarized in Fig. 2b. These values were calculated using a linear orthogonal distance regression analysis of correlation plots of discrete vs. fire-integrated ERs as shown in Fig. 3. The average slope and standard deviation is  $1.2 \pm 0.2$  indicating that the discrete ERs are generally higher than the fire-integrated ERs by 20 % on average. This positive bias is a consequence of the GC-MS sampling strategy which rarely included samples collected at the end of a burn (e.g.,  $t \geq 1000$  s in Fig. 1) when absolute emissions and ERs are lower for most species. Using the data in Fig. 1 as an example, 95 % of the emissions of benzene (in ppbv) occur between ignition and 1000 s, and the mean ER during this time is twice as large as the mean ER in the later portion of the fire (time = 1001 s to extinction). For VOCs emitted during the later stages of a fire (e.g., 1,3-benzenediol), the discrete ERs will likely underestimate the emissions relative to CO. For example, the discrete ERs for benzenediol for the southeastern and south-

western fuels (Table 2) are 30 % lower than the mean fire-integrated ERs reported by Veres et al. (2010).

The ability of the GC-MS to capture the fire-to-fire variability in VOC emissions relative to CO is evaluated by the strength of the correlation,  $r$ , between the discrete and fire-integrated ERs (Fig. 2b). Species with the weakest correlations, such as ethyne and benzene, show a distinct bifurcation that is dependent upon the MCE of the discrete samples (Fig. 3). These compounds have significant portion of emissions in both the flaming and smoldering phases of a fire (see Fig. 1). For these types of compounds, discrete samples collected in the smoldering phase (low MCE) did not adequately represent the fire-integrated emissions that include the intense flaming emissions (high MCE) resulting in poor correlation between discrete and fire-integrated ERs for these species. In contrast, VOCs that had the strongest correlations between the discrete and fire-integrated ERs (e.g., methanol and toluene where  $r > 0.88$ ) do not show a strong dependence on the MCE. Since CO is strongly associated with smoldering combustion (Yokelson et al., 1996; Burling et al., 2010), VOCs emitted primarily during this phase will be more tightly correlated with CO and the variability in the discrete vs. fire-integrated will be minimized.

In summary, the discrete GC-MS samples best characterize the fire-integrated emissions and fire-to fire variability of species produced primarily by smoldering combustion. We conservatively estimate these values to be within a factor of 1.5 of the fire-integrated ERs for the majority of the species measured. A similar conclusion was reached by comparing discrete ERs measured during the same fire to each other by Yokelson et al. (2013). While fire-integrated ERs are considered to best represent BB emissions, these analyses suggest that collecting and averaging multiple discrete ERs at various stages of the same or replicate burns, as presented here, are an adequate substitute when fire-integrated ERs cannot be determined. Fire-integrated ERs are commonly used to determine fuel-based emission factors for a fire, but care must be taken converting discrete ERs into emission factors, as also discussed for this data in Yokelson et al. (2013).

## Biomass burning emissions and potential air quality impacts

J. B. Gilman et al.

Title Page

Abstract

Introduction

Conclusions

References

Tables

Figures



Back

Close

Full Screen / Esc

Printer-friendly Version

Interactive Discussion



### 3.3 Characterization of laboratory BB emissions

In order to merge datasets from multiple instruments, we report mean discrete ERs of over 200 organic gases, including methane and VOCs, and 9 inorganic gases relative to CO for the southwestern, southeastern, and northern fuel types in the United States (Table 2). Mean ERs for each of the 18 individual fuel types are available at <http://www.esrl.noaa.gov/csd/groups/csd7/measurements/2009firelab/>. This study utilizes discrete ERs to characterize the chemical composition of the molar mass emitted, the VOC-OH reactivity, and the SOA potential of the measured emissions from fires simulating each fuel region in order to compare potential atmospheric impacts of these emissions and identify key species that may impact air quality through formation of O<sub>3</sub> and/or SOA.

Figure 4 is a pictograph of all ERs presented in Table 2 as well as a histogram of the ERs for each of the 3 fuel regions in order to highlight commonalities and differences in the magnitudes and general chemical composition of each simulated fuel region. The distribution of ERs are shown as a function of three simple properties including the degree of unsaturation ( $D = [2C + N - H + 2]/2$ , where C, N, and H denote the number of carbon, nitrogen, and hydrogen atoms, respectively); the number of oxygen atoms; and molecular weight (MW) of individual VOCs. Atmospheric lifetimes and fates of VOCs will depend, in part, on these properties, which we use as simplified proxies for reactivity (D), solubility (O-atoms), and volatility (MW). Using this general framework, we highlight several key features that will be explored in further detail in the subsequent sections:

- i. ERs are highly variable and span more than 4 orders of magnitude.
- ii. The relative magnitude and composition of the gases emitted are different for each of the 3 geographic fuel regions, i.e., the distribution of ERs are unique to each fuel region.

## Biomass burning emissions and potential air quality impacts

J. B. Gilman et al.

Title Page

Abstract

Introduction

Conclusions

References

Tables

Figures



Back

Close

Full Screen / Esc

Printer-friendly Version

Interactive Discussion



- iii. Southwestern fuels generally have lower ERs and northern fuels have the largest ERs. Collectively, the molar emission ratios are a factor of 3 greater for the northern fuels than the southwestern.
- iv. The largest ERs for all three fuel regions are associated with low molecular weight species ( $MW < 80 \text{ g mol}^{-1}$ ) and/or those that contain 1 or more oxygen atom(s). These species also have lower degrees of unsaturation ( $D \leq 2$ ) and populate the upper left quadrants of Fig. 4. VOCs with the largest ERs common to all fuel types are formaldehyde, ethene, acetic acid, and methanol (Table 2).
- v. Over 82 % of the molar emissions of VOCs from biomass burning are unsaturated compounds ( $D \geq 1$ ) defined as having one or more pi-bonds (e.g., C-C or C-O double bonds, cyclic or aromatic rings, etc.). In general, these species are more likely to react with atmospheric oxidants and/or photo-dissociate depending on the chemical moiety, making unsaturated species potentially important  $\text{O}_3$  and SOA precursors. VOCs that contain triple bonds (e.g., ethyne) are a notable exception as they tend to be less reactive.
- vi. The number of VOCs in the upper right quadrants of Fig. 4 (increasing ERs and degree of unsaturation) is greatest for northern fuels and least for southwestern fuels. Many of the VOCs in this quadrant also have relatively high molecular weights ( $MW \geq 100 \text{ g mol}^{-1}$ ) and most contain at least one oxygen atom (e.g., benzenediol and benzofuran). The combination of these physical properties indicate that these species are relatively reactive, soluble, and of low enough volatility to make them potentially important SOA precursors.

### 3.3.1 Molar mass emitted

Here we compare the magnitude and composition of biomass burning emissions as a function of molar mass, which is a readily calculated physical property used to quan-

## Biomass burning emissions and potential air quality impacts

J. B. Gilman et al.

Title Page

Abstract

Introduction

Conclusions

References

Tables

Figures



Back

Close

Full Screen / Esc

Printer-friendly Version

Interactive Discussion



tify BB emissions. Molar mass ( $\mu\text{g m}^{-3}$ ) emitted per ppmv CO is equal to:

$$\text{Molar Mass} = \sum \left( \frac{\text{ER} \cdot \text{MW}}{\text{MV}} \right) \quad (2)$$

where ER is the mean discrete emission ratio of a gas, MW is the molecular weight ( $\text{g mol}^{-1}$ ), and MV is molar volume (24.5 L at 1 atm and 25 °C). For all 3 fuel regions,  $\text{CO}_2$  was the overwhelmingly dominant gas-phase emission and singularly contributed over 95 % of the molar mass emitted. Collectively,  $\text{CH}_4$  and the inorganic gases (e.g.,  $\text{CO}_2$ , CO,  $\text{NO}_x$ , etc.) comprised over 99.05 % of all gaseous molar mass emitted and measured, while VOCs contributed only  $0.27 \pm 0.03$ ,  $0.34 \pm 0.03$ , and  $0.95 \pm 0.07$  % for the southeastern, southwestern, and northern fuels, respectively.

Figure 5a–c shows the fractional composition and total molar mass of measured VOCs emitted per ppmv CO for each fuel region. The molar mass emitted by northern fuels ( $324 \pm 22 \mu\text{g m}^{-3} \text{ ppmv CO}^{-1}$ ) is 3.5 times greater than the southwestern fuels ( $92 \pm 9 \mu\text{g m}^{-3} \text{ ppmv CO}^{-1}$ ). For all 3 fuel regions, the emissions are dominated by oxygen-containing VOCs (OVOCs), which collectively comprise 57–68 % of the total mass emissions. The largest contribution by a single chemical class is from OVOCs with low degrees of unsaturation ( $D \leq 1$ ), which contribute 29–40 % of the total molar mass emitted. This chemical family is dominated by acetic acid, formaldehyde, and methanol emissions (Table 2). Compared to hydrocarbons and OVOCs, nitrogen-containing VOCs are emitted in substantially smaller fractions, less than 8 % of the total. Dominant nitrogen VOCs include hydrocyanic acid (HCN), isocyanic acid (HNCO), acetonitrile ( $\text{CH}_3\text{CN}$ ), and methylnitrite ( $\text{CH}_3\text{ONO}$ ). The addition of all nitrogen-containing organics presented here would add approximately 5 % to the nitrogen budget presented in Burling et al. (2010); however, this would still leave over half of the fuel nitrogen potentially ending up in the ash, or being emitted as  $\text{N}_2$  or in other unmeasured gases based on the nitrogen content of the fuels which ranged from 0.48 to 1.3 %.

## Biomass burning emissions and potential air quality impacts

J. B. Gilman et al.

Title Page

Abstract

Introduction

Conclusions

References

Tables

Figures



Back

Close

Full Screen / Esc

Printer-friendly Version

Interactive Discussion



**Biomass burning emissions and potential air quality impacts**

J. B. Gilman et al.

[Title Page](#)[Abstract](#)[Introduction](#)[Conclusions](#)[References](#)[Tables](#)[Figures](#)[Back](#)[Close](#)[Full Screen / Esc](#)[Printer-friendly Version](#)[Interactive Discussion](#)

One limitation of this analysis is the exclusion of “unknown” species, which are (i) gaseous compounds that were measured but remain unidentified and were therefore omitted from this analysis because the chemical formula and family could not be properly identified or (ii) were undetectable by the suite of instruments listed in Table 1.

We estimate the mass contribution from the first scenario using the fuel-based emission factors compiled by Yokelson et al. (2013) for all measured species including “unknown” masses observed by the PIT-MS. These “unidentified” non-methane organic compounds (NMOC, equivalent to VOCs) accounted for 31–47 % of the mass emitted for the same fuels studied here (Yokelson et al., 2013). The second category of un-observed unknown species are likely to be of sufficiently high molecular weight, high polarity, and/or low volatility and thermal stability to escape detection by GC-MS, a variety of chemical ionization mass spectrometers, and the OP-FTIR. For example, BB emissions of species such as glyoxal, glycoaldehyde, acetol, guaiacols, syringols, and amines have been reported in the literature (McDonald et al., 2000; Schauer et al., 2001; McMeeking et al., 2009; Akagi et al., 2011, 2012; Hatch et al., 2015) but would not be detectable by any of the instruments used in this experiment. The contribution of these types of compounds is difficult to assess, so we roughly estimate an additional contribution of ~ 5 % to the total mass emitted could be from un-observed unknown VOCs. Collectively, we estimate that the species reported in Table 2 and compiled in Fig. 5a–c account for approximately 48–64 % of the expected mass of non-methane organic gases emitted from the fuels studied here. The total VOC molar mass emitted for each fuel type should be considered a lower limit and could increase by a factor of ~ 2. By extension, all of the totals presented in Fig. 5 should also be considered lower limits; however, the additional contribution of unidentified and/or un-measured species to the following discussions could not be determined.

### 3.3.2 OH reactivity of BB emissions

Oxidation of VOCs, often initiated by reaction with the hydroxyl radical ( $\bullet\text{OH}$ ), in the presence of  $\text{NO}_x$  ( $\text{NO} + \text{NO}_2$ ) leads to the photochemical formation of  $\text{O}_3$  and perox-



ynitrates, including peroxyacetic nitric anhydride (PAN). Due to the complex relationship between  $O_3$  production and VOC/ $NO_x$  ratios and peroxy nitrates, we use OH reactivity as a simplified metric to (i) compare the magnitude of reactive gases emitted by combustion of fuels characteristic of each region and to (ii) identify key reactive species that may contribute to the photochemical formation of  $O_3$  in a BB plume. Total OH reactivity represents the sum of all sinks of the hydroxyl radical ( $\bullet OH$ ) with all reactive gases and is equal to:

$$OH \text{ reactivity} = \sum (ER \cdot k_{OH} \cdot A) \quad (3)$$

where ER is the discrete emission ratio for each measured gases (VOCs,  $CH_4$ , CO,  $NO_2$ , and  $SO_2$ ; ppbv ( $\text{ppm CO}$ ) $^{-1}$ ),  $k_{OH}$  is the first-order reaction rate coefficient of a gas with the hydroxyl radical ( $\text{cm}^3 \text{ molec}^{-1} \text{ s}^{-1}$ ), and  $A$  is a molar concentration conversion factor ( $2.46 \times 10^{10} \text{ molec cm}^{-3} \text{ ppbv}^{-1}$  at 1 atm and 25°C). Reaction rate coefficients were compiled using the National Institute of Standards and Technology's Chemical Kinetics Database and the references therein (Manion et al., 2015). Based on the calculated OH reactivities of all measured species listed in Table 2, VOCs are the dominant sink of OH for all fuel regions contributing 70–90 ( $\pm 16$ )% of the total calculated OH reactivity even though non-methane VOCs were only 0.27–0.95% of the molar mass emitted.

Figure 5d–f shows the fractional contributions and total VOC-OH reactivities per ppmv CO for each of the 3 fuel regions. The fresh BB emissions from northern fuels have the highest OH reactivity ( $62 \pm 10 \text{ s}^{-1} \text{ ppmv CO}^{-1}$ ), which is 4.4 times greater than southwestern fuels ( $14 \pm 3 \text{ s}^{-1} \text{ ppmv CO}^{-1}$ ). Collectively, OVOCs provide the majority of the OH reactivity of the southeastern fuels (57%), while hydrocarbons dominate the southwestern (52%) and northern fuels (56%). Northern fuels have the largest contribution from highly reactive terpenes (14%) due to the ERs of these species being, on average, a factor of 5 greater than southeastern fuels and a factor of 40 greater than southwestern fuels.

## Biomass burning emissions and potential air quality impacts

J. B. Gilman et al.

Title Page

Abstract

Introduction

Conclusions

References

Tables

Figures

◀

▶

◀

▶

Back

Close

Full Screen / Esc

Printer-friendly Version

Interactive Discussion







BB plumes (Holzinger et al., 1999; de Gouw et al., 2003, 2006). Other more reactive nitrogen-containing organics including 2-propenenitrile, benzonitrile, and heterocyclic species such as pyrroles could serve as BB markers of fresh plumes (Friedli et al., 2001; Karl et al., 2007).

### 3.3.3 SOA potential of BB emissions

VOCs that are efficient SOA precursors are relatively reactive organic compounds whose oxidation products are of sufficiently low volatility or high solubility under some conditions. Aerosol yield is a measure of the mass of condensable compounds created from this oxidation per mass of VOC precursor; however, care must be taken to ensure that aerosol yields for various species were determined under comparable conditions (e.g., VOC: NO<sub>x</sub> ratios, oxidant concentrations, etc.). In order to conduct comparisons of SOA potential on a consistent scale, we use a model-based unitless metric developed by Derwent et al. (2010) that “reflects the propensity of VOCs to form SOA on an equal mass basis relative to toluene”. The photochemical transport model used to investigate SOA potentials (SOAPs) of 113 VOCs included explicit chemistry from the Master Chemical Mechanism (MCM v 3.1) using an idealized set of atmospheric conditions typical of a polluted urban boundary layer (Derwent et al., 2010). SOAPs were determined by the simulated mass of aerosol formed per mass of VOC reacted and is expressed relative to toluene (SOAP = 100). Species such as styrene and benzaldehyde have SOAP values of ~ 200 (i.e., twice as much potential SOA formed compared to toluene) and were used to estimate SOAPs for aromatics with unsaturated substituents, benzofurans, and benzenediols.

Figure 5g–i shows the composition and mean SOAPs of VOCs emitted for each of the 3 fuel regions. Southwestern fuels have the lowest SOA potential (480 per ppmv CO) compared to southeastern and northern fuels that have estimated SOAPs 2.7 and 5.1 times greater, respectively. Unsaturated OVOCs are the dominant fraction for all three fuel regions due to the relatively large ERs and SOAPs of benzenediols (sum of 1,2- and 1,3-), benzaldehyde, and phenols. Schauer et al. (2001) reports signifi-

## Biomass burning emissions and potential air quality impacts

J. B. Gilman et al.

Title Page

Abstract

Introduction

Conclusions

References

Tables

Figures



Back

Close

Full Screen / Esc

Printer-friendly Version

Interactive Discussion



**Biomass burning emissions and potential air quality impacts**

J. B. Gilman et al.

Title Page

Abstract

Introduction

Conclusions

References

Tables

Figures



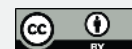
Back

Close

Full Screen / Esc

Printer-friendly Version

Interactive Discussion



cant gaseous emissions of benzenediols from combustion of pine in a fireplace and shows that 1,2-benzenediol (o-benzenediol) is the dominant gas-phase isomer while 1,3-benzenediol (m-benzenediol) is primarily associated with the particle phase. The discrete ERs used in this comparison may underestimate the emissions and SOA contribution of several compounds emitted in the later portions of a laboratory burn when emissions of most VOCs and CO were lower as previously discussed (Sect. 3.2).

The largest contributions to SOAP from hydrocarbons include aromatics with saturated functional groups (if any) such as benzene and toluene and aromatics with unsaturated substituents such as styrene. Traditionally, these are the species that are thought to be the largest contributors to SOA formation from urban emissions (Odum et al., 1997; Bahreini et al., 2012), although predicted SOA is typically much lower than observed in ambient air suggesting that the aerosol yields may be too low or there are additional SOA precursors that remain unaccounted for (de Gouw et al., 2005).

Monoterpenes have a very small ( $< 2\%$ ) contribution to total SOAP. The calculated SOAPs of monoterpenes are only 20% that of toluene (Derwent et al., 2010). This is in contrast to measured aerosol yields which are approximately 1.7 times higher for monoterpenes compared to toluene (Pandis et al., 1992). As a sensitivity test, we increased the SOAPs of the monoterpenes by a factor of 10 bringing the SOAP ratio of monoterpenes to toluene in line with that of measured aerosol yields. This resulted in modest increases in total SOAP of only 2% for SW and 5% for SE fuels. N fuels had the largest increase in total SOAP at 16%. With the adjusted monoterpene SOAPs, the fractional contribution of terpenes increased from 1.8% (Fig. 5i) to 15% of the total SOAP while the contribution of unsaturated OVOCs remained the dominant class but was reduced from 67 to 58% of the total SOAP. This sensitivity test suggests that the contributions of monoterpenes are likely underestimated for northern fuels if the SOAP scale is used; however, the largest contributions to SOAP for the northern fuels continues to be from oxygenated aromatics (benzenediols, phenols, and benzaldehyde). For comparison, Hatch et al. (2015) estimated that the SOA mass formed from the combustion of Ponderosa Pine is dominated by aromatic hydrocarbons (45%), terpenes



benzene, styrene, and methanol were enhanced in the BB plumes but are also present in urban emissions. An urban plume at 06:00–09:00 LT 9 September 2010 (Fig. 6) is enhanced in all of these species and CO; however, acetonitrile is not enhanced.

Observed enhancement ratios of several VOCs relative to acetonitrile and CO are compiled in Table 3 along with the types of emission sources for each VOC. Figure 7 shows a comparison of the VOC to acetonitrile ratios of select species for the Fourmile Canyon Fire and the laboratory-based biomass burns of all fuel types. We have identified benzofuran, 2-furaldehyde, 2-methylfuran, furan, and benzonitrile as the “best” tracers for BB emissions from these observations. These species (i) were well correlated with both acetonitrile and CO in the BB plumes, (ii) had negligible emissions from the urban and biogenic sources impacting the measurement site, and (iii) had large enhancements in BB plumes. In theory, the relative ratios of these species to acetonitrile may also be used as a BB-specific photochemical clock since each of these species represent a range of reactivities that are much greater than that of acetonitrile (Table 3). We compared the enhancement ratios of each VOC marker vs. acetonitrile for the two BB plumes observed on 9 August 2010 in order to determine if the relative age of the two BB plumes could be distinguished. While the enhancement ratios for several VOCs in each plume were statistically different from one another, there was no clear relationship between the observed differences in the enhancement ratios and the relative reactivity of the VOCs. Thus, small differences in the observed enhancement ratios more likely relate to differences in the fuel composition, the relative ratio of flaming vs. smoldering emissions in each BB plume, or variable secondary sources. Given enough time for significant photochemistry to occur as a BB plume moves further from the source, these ratios could be more useful to estimate photochemical ages.

## 4 Conclusions

We report a chemically detailed analysis of the trace gases emitted from burning 18 different biomass fuel types important in the southwestern, southeastern, and northern

## Biomass burning emissions and potential air quality impacts

J. B. Gilman et al.

Title Page

Abstract

Introduction

Conclusions

References

Tables

Figures



Back

Close

Full Screen / Esc

Printer-friendly Version

Interactive Discussion









## References

- Adler, G., Flores, J. M., Abo Riziq, A., Borrmann, S., and Rudich, Y.: Chemical, physical, and optical evolution of biomass burning aerosols: a case study, *Atmos. Chem. Phys.*, 11, 1491–1503, doi:10.5194/acp-11-1491-2011, 2011.
- 5 Akagi, S. K., Yokelson, R. J., Wiedinmyer, C., Alvarado, M. J., Reid, J. S., Karl, T., Crounse, J. D., and Wennberg, P. O.: Emission factors for open and domestic biomass burning for use in atmospheric models, *Atmos. Chem. Phys.*, 11, 4039–4072, doi:10.5194/acp-11-4039-2011, 2011.
- Akagi, S. K., Craven, J. S., Taylor, J. W., McMeeking, G. R., Yokelson, R. J., Burling, I. R.,  
10 Urbanski, S. P., Wold, C. E., Seinfeld, J. H., Coe, H., Alvarado, M. J., and Weise, D. R.: Evolution of trace gases and particles emitted by a chaparral fire in California, *Atmos. Chem. Phys.*, 12, 1397–1421, doi:10.5194/acp-12-1397-2012, 2012.
- Alvarado, M. J. and Prinn, R. G.: Formation of ozone and growth of aerosols in young smoke plumes from biomass burning: 1. Lagrangian parcel studies, *J. Geophys. Res.-Atmos.*, 114, D09306, doi:10.1029/2008jd011144, 2009.
- 15 Alvarado, M. J., Lonsdale, C. R., Yokelson, R. J., Akagi, S. K., Coe, H., Craven, J. S., Fischer, E. V., McMeeking, G. R., Seinfeld, J. H., Soni, T., Taylor, J. W., Weise, D. R., and Wold, C. E.: Investigating the links between ozone and organic aerosol chemistry in a biomass burning plume from a prescribed fire in California chaparral, *Atmos. Chem. Phys.*, 15, 6667–6688, doi:10.5194/acp-15-6667-2015, 2015.
- 20 Alvarez, E. G., Borrás, E., Viidanoja, J., and Hjorth, J.: Unsaturated dicarbonyl products from the OH-initiated photo-oxidation of furan, 2-methylfuran and 3-methylfuran, *Atmos. Environ.*, 43, 1603–1612, doi:10.1016/j.atmosenv.2008.12.019, 2009.
- Andreae, M. O. and Merlet, P.: Emission of trace gases and aerosols from biomass burning, *Global Biogeochem. Cy.*, 15, 955–966, 2001.
- 25 Bahreini, R., Middlebrook, A. M., de Gouw, J. A., Warneke, C., Trainer, M., Brock, C. A., Stark, H., Brown, S. S., Dube, W. P., Gilman, J. B., Hall, K., Holloway, J. S., Kuster, W. C., Perring, A. E., Prevot, A. S. H., Schwarz, J. P., Spackman, J. R., Szidat, S., Wagner, N. L., Weber, R. J., Zotter, P., and Parrish, D. D.: Gasoline emissions dominate over diesel in formation of secondary organic aerosol mass, *Geophys. Res. Lett.*, 39, L06805, doi:10.1029/2011gl050718, 2012.
- 30

## Biomass burning emissions and potential air quality impacts

J. B. Gilman et al.

Title Page

Abstract

Introduction

Conclusions

References

Tables

Figures



Back

Close

Full Screen / Esc

Printer-friendly Version

Interactive Discussion





**Biomass burning emissions and potential air quality impacts**

J. B. Gilman et al.

Title Page

Abstract

Introduction

Conclusions

References

Tables

Figures



Back

Close

Full Screen / Esc

Printer-friendly Version

Interactive Discussion

Bierbach, A., Barnes, I., and Becker, K. H.: Rate coefficients for the gas-phase reactions of hydroxyl radicals with furan, 2-methylfuran, 2-ethylfuran and 2,5-dimethylfuran at 300+/-2-K, *Atmos. Environ.*, 26, 813–817, 1992.

Bierbach, A., Barnes, I., and Becker, K. H.: Product and kinetic study of the oh-initiated gas-phase oxidation of furan, 2-methylfuran and furanaldehydes at  $\approx 300$  K, *Atmos. Environ.*, 29, 2651–2660, doi:10.1016/1352-2310(95)00096-H, 1995.

Burling, I. R., Yokelson, R. J., Griffith, D. W. T., Johnson, T. J., Veres, P., Roberts, J. M., Warneke, C., Urbanski, S. P., Reardon, J., Weise, D. R., Hao, W. M., and de Gouw, J.: Laboratory measurements of trace gas emissions from biomass burning of fuel types from the southeastern and southwestern United States, *Atmos. Chem. Phys.*, 10, 11115–11130, doi:10.5194/acp-10-11115-2010, 2010.

Burling, I. R., Yokelson, R. J., Akagi, S. K., Urbanski, S. P., Wold, C. E., Griffith, D. W. T., Johnson, T. J., Reardon, J., and Weise, D. R.: Airborne and ground-based measurements of the trace gases and particles emitted by prescribed fires in the United States, *Atmos. Chem. Phys.*, 11, 12197–12216, doi:10.5194/acp-11-12197-2011, 2011.

Christian, T. J., Kleiss, B., Yokelson, R. J., Holzinger, R., Crutzen, P. J., Hao, W. M., Saharjo, B. H., and Ward, D. E.: Comprehensive laboratory measurements of biomass-burning emissions: 1. Emissions from Indonesian, African, and other fuels, *J. Geophys. Res.-Atmos.*, 108, 4719, doi:10.1029/2003JD003704, 2003.

Christian, T. J., Kleiss, B., Yokelson, R. J., Holzinger, R., Crutzen, P. J., Hao, W. M., Shirai, T., and Blake, D. R.: Comprehensive laboratory measurements of biomass-burning emissions: 2. First intercomparison of open-path FTIR, PTR-MS, and GC-MS/FID/ECD, *J. Geophys. Res.-Atmos.*, 109, D02311, doi:10.1029/2003JD003874, 2004.

Crutzen, P. J. and Andreae, M. O.: Biomass burning in the Tropics – impact on atmospheric chemistry and biogeochemical cycles, *Science*, 250, 1669–1678, doi:10.1126/science.250.4988.1669, 1990.

de Gouw, J. A., Warneke, C., Parrish, D. D., Holloway, J. S., Trainer, M., and Fehsenfeld, F. C.: Emission sources and ocean uptake of acetonitrile ( $\text{CH}_3\text{CN}$ ) in the atmosphere, *J. Geophys. Res.-Atmos.*, 108, 4329, doi:10.1029/2002jd002897, 2003.

de Gouw, J. A., Middlebrook, A. M., Warneke, C., Goldan, P. D., Kuster, W. C., Roberts, J. M., Fehsenfeld, F. C., Worsnop, D. R., Canagaratna, M. R., Pszenny, A. A. P., Keene, W. C., Marchewka, M., Bertman, S. B., and Bates, T. S.: Budget of organic carbon in a polluted

## Biomass burning emissions and potential air quality impacts

J. B. Gilman et al.

[Title Page](#)

[Abstract](#)

[Introduction](#)

[Conclusions](#)

[References](#)

[Tables](#)

[Figures](#)



[Back](#)

[Close](#)

[Full Screen / Esc](#)

[Printer-friendly Version](#)

[Interactive Discussion](#)



- atmosphere: results from the New England Air Quality Study in 2002, *J. Geophys. Res.-Atmos.*, 110, D16305, doi:10.1029/2004JD005623, 2005.
- de Gouw, J. A., Warneke, C., Stohl, A., Wollny, A. G., Brock, C. A., Cooper, O. R., Holloway, J. S., Trainer, M., Fehsenfeld, F. C., Atlas, E. L., Donnelly, S. G., Stroud, V., and Lueb, A.: Volatile organic compounds composition of merged and aged forest fire plumes from Alaska and western Canada, *J. Geophys. Res.-Atmos.*, 111, D10303, doi:10.1029/2005JD006175, 2006.
- Demirbas, M. F. and Demirbas, T.: Hazardous emissions from combustion of biomass, *Energ. Source.*, 31, 527–534, doi:10.1080/15567030802466953, 2009.
- Derwent, R. G., Jenkin, M. E., Utembe, S. R., Shallcross, D. E., Murrells, T. P., and Passant, N. R.: Secondary organic aerosol formation from a large number of reactive man-made organic compounds, *Sci. Total Environ.*, 408, 3374–3381, doi:10.1016/j.scitotenv.2010.04.013, 2010.
- Estrellan, C. R. and Iino, F.: Toxic emissions from open burning, *Chemosphere*, 80, 193–207, doi:10.1016/j.chemosphere.2010.03.057, 2010.
- Fischer, E. V., Jacob, D. J., Yantosca, R. M., Sulprizio, M. P., Millet, D. B., Mao, J., Paulot, F., Singh, H. B., Roiger, A., Ries, L., Talbot, R.W., Dzepina, K., and Pandey Deolal, S.: Atmospheric peroxyacetyl nitrate (PAN): a global budget and source attribution, *Atmos. Chem. Phys.*, 14, 2679–2698, doi:10.5194/acp-14-2679-2014, 2014.
- Friedli, H. R., Atlas, E., Stroud, V. R., Giovanni, L., Campos, T., and Radke, L. F.: Volatile organic trace gases emitted from North American wildfires, *Global Biogeochem. Cy.*, 15, 435–452, 2001.
- Gerbig, C., Schmitgen, S., Kley, D., Volz-Thomas, A., Dewey, K., and Haaks, D.: An improved fast-response vacuum-UV resonance fluorescence CO instrument, *J. Geophys. Res.-Atmos.*, 104, 1699–1704, 1999.
- Gilman, J. B., Kuster, W. C., Goldan, P. D., Herndon, S. C., Zahniser, M. S., Tucker, S. C., Brewer, W. A., Lerner, B. M., Williams, E. J., Harley, R. A., Fehsenfeld, F. C., Warneke, C., and de Gouw, J. A.: Measurements of volatile organic compounds during the 2006 TexAQS/GoMACCS campaign: industrial influences, regional characteristics, and diurnal dependencies of the OH reactivity, *J. Geophys. Res.-Atmos.*, 114, D00F06, doi:10.1029/2008jd011525, 2009.
- Gilman, J. B., Burkhardt, J. F., Lerner, B. M., Williams, E. J., Kuster, W. C., Goldan, P. D., Murphy, P. C., Warneke, C., Fowler, C., Montzka, S. A., Miller, B. R., Miller, L., Oltmans, S. J., Ryerson, T. B., Cooper, O. R., Stohl, A., and de Gouw, J. A.: Ozone variability and halogen

## Biomass burning emissions and potential air quality impacts

J. B. Gilman et al.

Title Page

Abstract

Introduction

Conclusions

References

Tables

Figures



Back

Close

Full Screen / Esc

Printer-friendly Version

Interactive Discussion



oxidation within the Arctic and sub-Arctic springtime boundary layer, *Atmos. Chem. Phys.*, 10, 10223–10236, doi:10.5194/acp-10-10223-2010, 2010.

Goldan, P. D., Kuster, W. C., Williams, E., Murphy, P. C., Fehsenfeld, F. C., and Meagher, J.: Nonmethane hydrocarbon and oxy hydrocarbon measurements during the 2002 New England Air Quality Study, *J. Geophys. Res.-Atmos.*, 109, D21309, doi:10.1029/2003JD004455, 2004.

Hatch, L. E., Luo, W., Pankow, J. F., Yokelson, R. J., Stockwell, C. E., and Barsanti, K. C.: Identification and quantification of gaseous organic compounds emitted from biomass burning using two-dimensional gas chromatography–time-of-flight mass spectrometry, *Atmos. Chem. Phys.*, 15, 1865–1899, doi:10.5194/acp-15-1865-2015, 2015.

Hegg, D. A., Radke, L. F., Hobbs, P. V., Rasmussen, R. A., and Riggan, P. J.: Emissions of some trace gases from biomass fires, *J. Geophys. Res.-Atmos.*, 95, 5669–5675, doi:10.1029/JD095iD05p05669, 1990.

Heilman, W. E., Liu, Y., Urbanski, S., Kovalev, V., and Mickler, R.: Wildland fire emissions, carbon, and climate: plume rise, atmospheric transport, and chemistry processes, *Forest Ecol. Manag.*, 317, 70–79, doi:10.1016/j.foreco.2013.02.001, 2014.

Holzinger, R., Warneke, C., Hansel, A., Jordan, A., Lindinger, W., Scharffe, D. H., Schade, G., and Crutzen, P. J.: Biomass burning as a source of formaldehyde, acetaldehyde, methanol, acetone, acetonitrile, and hydrogen cyanide, *Geophys. Res. Lett.*, 26, 1161–1164, doi:10.1029/1999gl900156, 1999.

Jaffe, D. A. and Wigder, N. L.: Ozone production from wildfires: a critical review, *Atmos. Environ.*, 51, 1–10, doi:10.1016/j.atmosenv.2011.11.063, 2012.

Karl, T. G., Christian, T. J., Yokelson, R. J., Artaxo, P., Hao, W. M., and Guenther, A.: The Tropical Forest and Fire Emissions Experiment: method evaluation of volatile organic compound emissions measured by PTR-MS, FTIR, and GC from tropical biomass burning, *Atmos. Chem. Phys.*, 7, 5883–5897, doi:10.5194/acp-7-5883-2007, 2007.

Kroll, J. H. and Seinfeld, J. H.: Chemistry of secondary organic aerosol: formation and evolution of low-volatility organics in the atmosphere, *Atmos. Environ.*, 42, 3593–3624, doi:10.1016/j.atmosenv.2008.01.003, 2008.

Manion, J. A., Huie, R. E., Levin, R. D., Burgess Jr., D. R., Orkin, V. L., Tsang, W., McGivern, W. S., Hudgens, J. W., Knyazev, V. D., Atkinson, D. B., Chai, E., Tereza, A. M., Lin, C. J., Allison, T. C., Mallard, W. G., Westley, F., Herron, J. T., Hampson, R. F., and

**Biomass burning emissions and potential air quality impacts**

J. B. Gilman et al.

Title Page

Abstract

Introduction

Conclusions

References

Tables

Figures



Back

Close

Full Screen / Esc

Printer-friendly Version

Interactive Discussion



Frizzell, D. H.: NIST Standard Reference Database 17, Version 7.0, Web Version available at: <http://kinetics.nist.gov/> (last access: 21 February 2015), 2015.

Mason, S. A., Trentmann, J., Winterrath, T., Yokelson, R. J., Christian, T. J., Carlson, L. J., Warner, T. R., Wolfe, L. C., and Andreae, M. O.: Intercomparison of two box models of the chemical evolution in biomass-burning smoke plumes, *J. Atmos. Chem.*, 55, 273–297, doi:10.1007/s10874-006-9039-5, 2006.

McDonald, J. D., Zielinska, B., Fujita, E. M., Sagebiel, J. C., Chow, J. C., and Watson, J. G.: Fine particle and gaseous emission rates from residential wood combustion, *Environ. Sci. Technol.*, 34, 2080–2091, doi:10.1021/es9909632, 2000.

McMeeking, G. R., Kreidenweis, S. M., Baker, S., Carrico, C. M., Chow, J. C., Collett, J. L., Hao, W. M., Holden, A. S., Kirchstetter, T. W., Malm, W. C., Moosmuller, H., Sullivan, A. P., and Wold, C. E.: Emissions of trace gases and aerosols during the open combustion of biomass in the laboratory, *J. Geophys. Res.-Atmos.*, 114, D19210, doi:10.1029/2009jd011836, 2009.

Odum, J. R., Jungkamp, T. P. W., Griffin, R. J., Flagan, R. C., and Seinfeld, J. H.: The atmospheric aerosol-forming potential of whole gasoline vapor, *Science*, 276, 96–99, 1997.

Pandis, S. N., Harley, R. A., Cass, G. R., and Seinfeld, J. H.: Secondary organic aerosol formation and transport, *Atmos. Environ.*, 26, 2269–2282, 1992.

Pankow, J. F.: An absorption model of the gas-aerosol partitioning involved in the formation of secondary organic aerosol, *Atmos. Environ.*, 28, 189–193, doi:10.1016/1352-2310(94)90094-9, 1994.

Roberts, J. M., Marchewka, M., Bertman, S. B., Sommariva, R., Warneke, C., de Gouw, J., Kuster, W., Goldan, P., Williams, E., Lerner, B. M., Murphy, P., and Fehsenfeld, F. C.: Measurements of PANs during the New England air quality study 2002, *J. Geophys. Res.-Atmos.*, 112, D20306, doi:10.1029/2007JD008667, 2007.

Roberts, J. M., Veres, P., Warneke, C., Neuman, J. A., Washenfelder, R. A., Brown, S. S., Baasandorj, M., Burkholder, J. B., Burling, I. R., Johnson, T. J., Yokelson, R. J., and de Gouw, J.: Measurement of HONO, HNCO, and other inorganic acids by negative-ion proton-transfer chemical-ionization mass spectrometry (NI-PT-CIMS): application to biomass burning emissions, *Atmos. Meas. Tech.*, 3, 981–990, doi:10.5194/amt-3-981-2010, 2010.

Roberts, J. M., Veres, P. R., Cochran, A. K., Warneke, C., Burling, I. R., Yokelson, R. J., Lerner, B., Gilman, J. B., Kuster, W. C., Fall, R., and de Gouw, J.: Isocyanic acid in the atmosphere and its possible link to smoke-related health effects, *P. Natl. Acad. Sci. USA*, 108, 8966–8971, doi:10.1073/pnas.1103352108, 2011.

## Biomass burning emissions and potential air quality impacts

J. B. Gilman et al.

Title Page

Abstract

Introduction

Conclusions

References

Tables

Figures



Back

Close

Full Screen / Esc

Printer-friendly Version

Interactive Discussion



Schauer, J. J., Kleeman, M. J., Cass, G. R., and Simoneit, B. R. T.: Measurement of emissions from air pollution sources. 3. C-1-C-29 organic compounds from fireplace combustion of wood, *Environ. Sci. Technol.*, 35, 1716–1728, doi:10.1021/es001331e, 2001.

Simpson, I. J., Akagi, S. K., Barletta, B., Blake, N. J., Choi, Y., Diskin, G. S., Fried, A., Fuelberg, H. E., Meinardi, S., Rowland, F. S., Vay, S. A., Weinheimer, A. J., Wennberg, P. O., Wiebring, P., Wisthaler, A., Yang, M., Yokelson, R. J., and Blake, D. R.: Boreal forest fire emissions in fresh Canadian smoke plumes: C<sub>1</sub>-C<sub>10</sub> volatile organic compounds (VOCs), CO<sub>2</sub>, CO, NO<sub>2</sub>, NO, HCN and CH<sub>3</sub>CN, *Atmos. Chem. Phys.*, 11, 6445–6463, doi:10.5194/acp-11-6445-2011, 2011.

Sommers, W. T., Loehman, R. A., and Hardy, C. C.: Wildland fire emissions, carbon, and climate: science overview and knowledge needs, *Forest Ecol. Manag.*, 317, 1–8, doi:10.1016/j.foreco.2013.12.014, 2014.

Stockwell, C. E., Yokelson, R. J., Kreidenweis, S. M., Robinson, A. L., DeMott, P. J., Sullivan, R. C., Reardon, J., Ryan, K. C., Griffith, D. W. T., and Stevens, L.: Trace gas emissions from combustion of peat, crop residue, domestic biofuels, grasses, and other fuels: configuration and Fourier transform infrared (FTIR) component of the fourth Fire Lab at Missoula Experiment (FLAME-4), *Atmos. Chem. Phys.*, 14, 9727–9754, doi:10.5194/acp-14-9727-2014, 2014.

Stockwell, C. E., Veres, P. R., Williams, J., and Yokelson, R. J.: Characterization of biomass burning emissions from cooking fires, peat, crop residue, and other fuels with high-resolution proton-transfer-reaction time-of-flight mass spectrometry, *Atmos. Chem. Phys.*, 15, 845–865, doi:10.5194/acp-15-845-2015, 2015.

Trentmann, J., Andreae, M. O., and Graf, H. F.: Chemical processes in a young biomass-burning plume, *J. Geophys. Res.-Atmos.*, 108, 4705–4714, doi:10.1029/2003jd003732, 2003.

Trentmann, J., Yokelson, R. J., Hobbs, P. V., Winterrath, T., Christian, T. J., Andreae, M. O., and Mason, S. A.: An analysis of the chemical processes in the smoke plume from a savanna fire, *J. Geophys. Res.-Atmos.*, 110, D12301, doi:10.1029/2004jd005628, 2005.

Tuazon, E. C., Alvarado, A., Aschmann, S. M., Atkinson, R., and Arey, J.: Products of the gas-phase reactions of 1,3-butadiene with OH and NO<sub>3</sub> Radicals, *Environ. Sci. Technol.*, 33, 3586–3595, doi:10.1021/es990193u, 1999.

Urbanski, S.: Wildland fire emissions, carbon, and climate: emission factors, *Forest. Ecol. Manag.*, 317, 51–60, doi:10.1016/j.foreco.2013.05.045, 2014.

**Biomass burning emissions and potential air quality impacts**

J. B. Gilman et al.

Title Page

Abstract

Introduction

Conclusions

References

Tables

Figures



Back

Close

Full Screen / Esc

Printer-friendly Version

Interactive Discussion



- Veres, P., Roberts, J. M., Burling, I. R., Warneke, C., de Gouw, J., and Yokelson, R. J.: Measurements of gas-phase inorganic and organic acids from biomass fires by negative-ion proton-transfer chemical-ionization mass spectrometry, *J. Geophys. Res.-Atmos.*, 115, D23302, doi:10.1029/2010jd014033, 2010.
- 5 Warneke, C., Roberts, J. M., Veres, P., Gilman, J., Kuster, W. C., Burling, I., Yokelson, R., and de Gouw, J. A.: VOC identification and inter-comparison from laboratory biomass burning using PTR-MS and PIT-MS, *Int. J. Mass Spectrom.*, 303, 6–14, doi:10.1016/j.ijms.2010.12.002, 2011.
- Yokelson, R. J., Griffith, D. W. T., and Ward, D. E.: Open-path Fourier transform infrared studies of large-scale laboratory biomass fires, *J. Geophys. Res.-Atmos.*, 101, 21067–21080, 1996.
- 10 Yokelson, R. J., Burling, I. R., Gilman, J. B., Warneke, C., Stockwell, C. E., de Gouw, J., Akagi, S. K., Urbanski, S. P., Veres, P., Roberts, J. M., Kuster, W. C., Reardon, J., Griffith, D. W. T., Johnson, T. J., Hosseini, S., Miller, J. W., Cocker III, D. R., Jung, H., and Weise, D. R.: Coupling field and laboratory measurements to estimate the emission factors of identified and unidentified trace gases for prescribed fires, *Atmos. Chem. Phys.*, 13, 89–116, doi:10.5194/acp-13-89-2013, 2013.
- 15

## Biomass burning emissions and potential air quality impacts

J. B. Gilman et al.

Title Page

Abstract

Introduction

Conclusions

References

Tables

Figures

◀

▶

◀

▶

Back

Close

Full Screen / Esc

Printer-friendly Version

Interactive Discussion



**Table 1.** Instrument description.

| Name              | Instrument  | Meas. Description  | Sampling Limitations   | References                                   |
|-------------------|---|--|--|--|
| <b>GC-MS</b>      | <i>Gas chromatograph-(Quadrupole) Mass Spectrometer</i>                     | Discrete sampling via cryogenic pre-concentration, chromatographic separation, and identification via retention time and electron impact ionization mass spectrum  | Melting point > $-185^{\circ}\text{C}$<br>boiling point < $220^{\circ}\text{C}$<br>sufficiently non-polar<br>mass frag. ( $m/z$ ): 26 to 150 a.m.u       | Goldan et al. (2004)<br>Gilman et al. (2010) |
| <b>PTR-MS</b>     | <i>Proton Transfer Reaction-(Quadrupole) Mass Spectrometer</i>              | Real-time sampling via proton transfer reactions with $\text{H}_3\text{O}^+$ and identification via protonated ion ( $\text{M} + \text{H}$ ) <sup>+</sup> with quadrupole mass filter                      | Proton affinity greater than water; Protonated molecular mass or mass fragment ( $m/z$ ): 20–240 a.m.u   | Warneke et al. (2011)                        |
| <b>PIT-MS</b>     | <i>Proton Transfer Reaction-(Ion Trap) Mass Spectrometer</i>                | Real-time sampling via proton transfer reactions with $\text{H}_3\text{O}^+$ and identification via protonated ion ( $\text{M} + \text{H}$ ) <sup>+</sup> with ion trap mass spectrometer                  | Proton affinity greater than water; Protonated molecular mass or mass fragment ( $m/z$ ): 20–240 a.m.u   | Warneke et al. (2011)                        |
| <b>NI-PT-CIMS</b> | <i>Negative Ion-Proton Transfer Reaction-(Quadrupole) Mass Spectrometer</i> | Real-time sampling via proton transfer reactions with $\text{CH}_3\text{C}(\text{O})\text{O}^-$ and identification via deprotonated ion ( $\text{M} - \text{H}$ ) <sup>-</sup> with quadrupole mass filter | Gas-phase acidity greater than that of acetic acid; Deprotonated molecular mass or mass fragment ( $m/z$ ): 10–225 a.m.u                                 | Veres et al. (2011)<br>Roberts et al. (2011) |
| <b>OP-FTIR</b>    | <i>Open Path-Fourier Transform Infrared Spectrometer</i>                    | Real-time spectral scanning via open path White cell, offline identification via compound specific infrared absorption features  | Strong absorption features between $600\text{--}3400\text{ cm}^{-1}$ that are unique and have minimal interferences from other strong infrared-absorbers | Burling et al. (2011)                        |

## Biomass burning emissions and potential air quality impacts

J. B. Gilman et al.

Title Page

Abstract

Introduction

Conclusions

References

Tables

Figures

⏪

⏩

◀

▶

Back

Close

Full Screen / Esc

Printer-friendly Version

Interactive Discussion

**Table 2.** Mean VOC to CO discrete emission ratios (ERs) for the southwestern (SW), south-eastern (SE), and northern (N) fuel regions.

| Name                              | Formula                         | MW  | D | m/z | SW Avg        | (±SD)    | npnts | SE Avg        | (±SD)    | npnts | N Avg          | (±SD)     | npnts |
|-----------------------------------|---------------------------------|-----|---|-----|---------------|----------|-------|---------------|----------|-------|----------------|-----------|-------|
| <b>Alkanes (Saturated, D = 0)</b> |                                 |     |   |     |               |          |       |               |          |       |                |           |       |
| Ethane                            | C <sub>2</sub> H <sub>6</sub>   | 30  | 0 | 27  | <b>1.8388</b> | (1.2846) | 25    | <b>4.5311</b> | (3.8024) | 23    | <b>6.8510</b>  | (3.5152)  | 4     |
| Propane                           | C <sub>3</sub> H <sub>8</sub>   | 44  | 0 | 27  | <b>0.6317</b> | (0.9985) | 23    | <b>1.5957</b> | (1.2193) | 18    | <b>1.4633</b>  | (0.9354)  | 4     |
| Butane_iso                        | C <sub>4</sub> H <sub>10</sub>  | 58  | 0 | 43  | 0.0522        | (0.0813) | 29    | 0.2984        | (0.4734) | 20    | 0.0982         | (0.0620)  | 4     |
| Butane_n                          | C <sub>4</sub> H <sub>10</sub>  | 58  | 0 | 43  | <b>0.1038</b> | (0.1829) | 29    | <b>0.3333</b> | (0.2902) | 20    | <b>0.4005</b>  | (0.2804)  | 4     |
| Propane_2dimethyl                 | C <sub>5</sub> H <sub>12</sub>  | 72  | 0 | 57  | 0.0003        | (0.0008) | 29    | 0.0004        | (0.0008) | 23    | 0.0006         | (0.0007)  | 4     |
| Pentane_iso                       | C <sub>5</sub> H <sub>12</sub>  | 72  | 0 | 43  | 0.0167        | (0.0585) | 29    | 0.0580        | (0.0878) | 23    | 0.0322         | (0.0261)  | 4     |
| Pentane_n                         | C <sub>5</sub> H <sub>12</sub>  | 72  | 0 | 43  | 0.0271        | (0.0427) | 29    | 0.0889        | (0.0789) | 23    | 0.1400         | (0.1130)  | 4     |
| Butane_2dimethyl                  | C <sub>6</sub> H <sub>14</sub>  | 86  | 0 | 71  | 0.0002        | (0.0008) | 29    | 0.0001        | (0.0002) | 23    |                |           | 0     |
| Pentane_3methyl                   | C <sub>6</sub> H <sub>14</sub>  | 86  | 0 | 57  | 0.0009        | (0.0010) | 9     | 0.0089        | (0.0117) | 16    | 0.0045         | (0.0031)  | 4     |
| Hexane_n                          | C <sub>6</sub> H <sub>14</sub>  | 86  | 0 | 57  | 0.0159        | (0.0225) | 29    | 0.0572        | (0.0516) | 23    | 0.0814         | (0.0634)  | 4     |
| Heptane_n                         | C <sub>7</sub> H <sub>16</sub>  | 100 | 0 | 43  | 0.0218        | (0.0176) | 9     | 0.0640        | (0.0387) | 14    | 0.0836         | (0.0674)  | 4     |
| Octane_n                          | C <sub>8</sub> H <sub>18</sub>  | 114 | 0 | 43  | 0.0138        | (0.0128) | 9     | 0.0469        | (0.0281) | 14    | 0.0536         | (0.0353)  | 4     |
| Nonane_n                          | C <sub>9</sub> H <sub>20</sub>  | 128 | 0 | 57  | 0.0085        | (0.0079) | 9     | 0.0358        | (0.0213) | 13    | 0.0369         | (0.0269)  | 4     |
| Decane_n                          | C <sub>10</sub> H <sub>22</sub> | 142 | 0 | 57  | 0.0083        | (0.0060) | 9     | 0.0310        | (0.0222) | 14    | 0.0330         | (0.0212)  | 4     |
| Undecane_n                        | C <sub>11</sub> H <sub>24</sub> | 156 | 0 | 57  | 0.0111        | (0.0054) | 8     | 0.0412        | (0.0304) | 12    | 0.0425         | (0.0208)  | 4     |
| <b>Alkenes (Saturated, D = 1)</b> |                                 |     |   |     |               |          |       |               |          |       |                |           |       |
| Ethene                            | C <sub>2</sub> H <sub>4</sub>   | 28  | 1 | 27  | <b>5.8525</b> | (4.1077) | 25    | <b>8.1879</b> | (4.2382) | 21    | <b>18.3160</b> | (12.8430) | 4     |
| Propene                           | C <sub>3</sub> H <sub>6</sub>   | 42  | 1 | 41  | <b>2.0801</b> | (2.0528) | 29    | <b>3.4917</b> | (2.1610) | 23    | <b>8.5115</b>  | (3.4340)  | 4     |
| Propene_2methyl                   | C <sub>4</sub> H <sub>8</sub>   | 56  | 1 | 41  | 0.1046        | (0.1652) | 29    | 0.2668        | (0.2151) | 23    | 0.3162         | (0.3624)  | 4     |
| Butene_1                          | C <sub>4</sub> H <sub>8</sub>   | 56  | 1 | 41  | <b>0.2961</b> | (0.3761) | 29    | <b>0.4851</b> | (0.3320) | 23    | <b>1.5227</b>  | (0.6632)  | 4     |
| Butene_cis2                       | C <sub>4</sub> H <sub>8</sub>   | 56  | 1 | 41  | 0.0579        | (0.0937) | 29    | 0.1209        | (0.0920) | 23    | 0.2397         | (0.1916)  | 4     |
| Butene_trans2                     | C <sub>4</sub> H <sub>8</sub>   | 56  | 1 | 41  | 0.0615        | (0.1036) | 29    | 0.1427        | (0.1174) | 23    | 0.2732         | (0.2648)  | 4     |
| Butene_1_3methyl                  | C <sub>5</sub> H <sub>10</sub>  | 70  | 1 | 55  | 0.0202        | (0.0256) | 29    | 0.0391        | (0.0284) | 23    | 0.0681         | (0.0462)  | 4     |
| Butene_1_3methyl                  | C <sub>5</sub> H <sub>10</sub>  | 70  | 1 | 55  | 0.0091        | (0.0202) | 8     | 0.0152        | (0.0168) | 15    | 0.0183         | (0.0164)  | 4     |
| Butene_2_2methyl                  | C <sub>5</sub> H <sub>10</sub>  | 70  | 1 | 55  | 0.0224        | (0.0317) | 8     | 0.0996        | (0.0634) | 14    | 0.1881         | (0.0965)  | 4     |
| Cyclopentane                      | C <sub>5</sub> H <sub>10</sub>  | 70  | 1 | 42  | 0.0024        | (0.0040) | 29    | 0.0064        | (0.0053) | 23    | 0.0108         | (0.0074)  | 4     |
| Pentene_1                         | C <sub>5</sub> H <sub>10</sub>  | 70  | 1 | 55  | 0.0429        | (0.0654) | 29    | 0.0902        | (0.0773) | 23    | 0.2311         | (0.1872)  | 4     |
| Pentene_cis2                      | C <sub>5</sub> H <sub>10</sub>  | 70  | 1 | 55  | 0.0432        | (0.0638) | 8     | 0.1396        | (0.0883) | 14    | 0.2905         | (0.1492)  | 4     |
| Pentene_trans2                    | C <sub>5</sub> H <sub>10</sub>  | 70  | 1 | 55  | 0.0276        | (0.0341) | 29    | 0.0422        | (0.0304) | 23    | 0.1180         | (0.0667)  | 4     |
| Cyclopentane_1methyl              | C <sub>6</sub> H <sub>12</sub>  | 84  | 1 | 56  | 0.0040        | (0.0037) | 9     | 0.0147        | (0.0139) | 16    | 0.0159         | (0.0113)  | 4     |
| Pentene_1                         | C <sub>6</sub> H <sub>12</sub>  | 84  | 1 | 56  | 0.0890        | (0.1102) | 9     | 0.1782        | (0.1162) | 14    | 0.4980         | (0.2945)  | 4     |
| Cyclohexane                       | C <sub>6</sub> H <sub>12</sub>  | 84  | 1 | 84  | 0.0012        | (0.0014) | 9     | 0.0052        | (0.0028) | 14    | 0.0052         | (0.0035)  | 4     |
| Hexene_1                          | C <sub>6</sub> H <sub>12</sub>  | 84  | 1 | 84  | 0.1029        | (0.1182) | 8     | 0.2039        | (0.0943) | 12    | 0.4904         | (0.2844)  | 4     |
| Hexene_cis2                       | C <sub>6</sub> H <sub>12</sub>  | 84  | 1 | 84  | 0.0256        | (0.0338) | 9     | 0.0522        | (0.0443) | 16    | 0.1552         | (0.0586)  | 4     |
| Hexenes (sum of 3 isomers)        | C <sub>6</sub> H <sub>12</sub>  | 84  | 1 | 84  | 0.0931        | (0.1166) | 9     | 0.1788        | (0.1376) | 16    | 0.5432         | (0.2920)  | 4     |
| Cyclohexane_methyl                | C <sub>7</sub> H <sub>14</sub>  | 98  | 1 | 83  | 0.0023        | (0.0023) | 8     | 0.0097        | (0.0063) | 14    | 0.0111         | (0.0071)  | 4     |
| C <sub>7</sub> H <sub>14</sub>    | C <sub>7</sub> H <sub>14</sub>  | 98  | 1 | 56  | 0.0547        | (0.0595) | 9     | 0.1168        | (0.0721) | 14    | 0.2868         | (0.1559)  | 4     |
| Octene_1                          | C <sub>8</sub> H <sub>16</sub>  | 112 | 1 | 55  | 0.0431        | (0.0486) | 9     | 0.1013        | (0.0482) | 13    | 0.1651         | (0.0926)  | 4     |
| Nonene_1                          | C <sub>9</sub> H <sub>18</sub>  | 126 | 1 | 41  | 0.0097        | (0.0122) | 9     | 0.0196        | (0.0153) | 16    | 0.0474         | (0.0326)  | 4     |
| Decene_1                          | C <sub>10</sub> H <sub>20</sub> | 140 | 1 | 56  | 0.0133        | (0.0159) | 9     | 0.0260        | (0.0228) | 16    | 0.0812         | (0.0415)  | 4     |
| Undecene_1                        | C <sub>11</sub> H <sub>22</sub> | 154 | 1 | 55  | 0.0103        | (0.0100) | 9     | 0.0279        | (0.0292) | 16    | 0.0647         | (0.0251)  | 4     |



# Biomass burning emissions and potential air quality impacts

J. B. Gilman et al.

Title Page

Abstract

Introduction

Conclusions

References

Tables

Figures



Back

Close

Full Screen / Esc

Printer-friendly Version

Interactive Discussion



Table 2. Continued.

| Name   | Formula | MW  | D | m/z  | SW Avg        | (±SD)    | npnts | SE Avg        | (±SD)    | npnts | N Avg         | (±SD)    | npnts |
|--|---------|-----|---|------|---------------|----------|-------|---------------|----------|-------|---------------|----------|-------|
| <b>Alkynes and Alkenes (Polyunsaturated, D &gt; 0)</b> |         |     |   |      |               |          |       |               |          |       |               |          |       |
| Ethyne   | C2H2    | 26  | 2 | 1R   | <b>2.3905</b> | (3.0119) | 27    | <b>1.7412</b> | (1.3580) | 23    | <b>5.0910</b> | (5.6894) | 4     |
| Propyne  | C3H4    | 40  | 2 | 39   | <b>0.2093</b> | (0.1503) | 29    | <b>0.1850</b> | (0.1626) | 23    | <b>0.7876</b> | (0.6405) | 4     |
| Butadiyne_13 (Diacetylene)                             | C4H2    | 50  | 4 | 50   | 0.0080        | (0.0054) | 9     | 0.0041        | (0.0052) | 16    | 0.0427        | (0.0651) | 4     |
| Butenyne (Vinylacetylene)                              | C4H4    | 52  | 3 | 52   | 0.0285        | (0.0452) | 9     | 0.0154        | (0.0190) | 16    | 0.0824        | (0.1062) | 4     |
| Butadiene_12   | C4H6    | 54  | 2 | 54   | 0.0101        | (0.0146) | 29    | 0.0087        | (0.0095) | 23    | 0.0441        | (0.0343) | 4     |
| Butadiene_13   | C4H6    | 54  | 2 | 54   | <b>0.4065</b> | (0.5315) | 29    | <b>0.4122</b> | (0.3530) | 23    | <b>1.8781</b> | (0.9509) | 4     |
| Butyne (1- or 2-)                                      | C4H6    | 54  | 2 | 54   | 0.0221        | (0.0287) | 9     | 0.0158        | (0.0146) | 16    | 0.0693        | (0.0300) | 4     |
| Cyclopentadiene_13                                     | C5H6    | 66  | 3 | 66   | 0.1724        | (0.3868) | 8     | 0.1747        | (0.0992) | 14    | 0.5836        | (0.3458) | 4     |
| Pentenyne isomer (e.g., propenylacetylene)             | C5H6    | 66  | 3 | 66   | 0.0161        | (0.0176) | 9     | 0.0107        | (0.0119) | 16    | 0.0651        | (0.0395) | 4     |
| Butyne_3methyl   | C5H8    | 68  | 2 | 67   | 0.0090        | (0.0166) | 9     | 0.0103        | (0.0108) | 16    | 0.0426        | (0.0303) | 4     |
| Cyclopentene   | C5H8    | 68  | 2 | 67   | 0.0699        | (0.1240) | 7     | 0.1125        | (0.0789) | 14    | 0.2815        | (0.1725) | 4     |
| Pentadiene_cis13                                       | C5H8    | 68  | 2 | 67   | 0.0457        | (0.0795) | 8     | 0.0627        | (0.0360) | 14    | 0.1733        | (0.0691) | 4     |
| Pentadiene_trans13                                     | C5H8    | 68  | 2 | 67   | 0.0668        | (0.1069) | 9     | 0.1044        | (0.0538) | 14    | 0.2504        | (0.0927) | 4     |
| Hexadienyne (e.g., divinylacetylene)                   | C6H6    | 78  | 4 | 78   | 0.0140        | (0.0152) | 9     | 0.0088        | (0.0072) | 16    | 0.0569        | (0.0382) | 4     |
| Cyclopentadiene_methyl (sum of 2 isomers)              | C6H8    | 80  | 3 | 79   | 0.0242        | (0.0329) | 9     | 0.0516        | (0.0554) | 16    | 0.1831        | (0.1771) | 4     |
| Hexenyne (e.g., 2-methyl- 1-penten-3-yne)              | C6H8    | 80  | 3 | 80   | 0.0110        | (0.0127) | 9     | 0.0102        | (0.0117) | 16    | 0.0674        | (0.0545) | 4     |
| Cyclohexene  | C6H10   | 82  | 2 | 67   | 0.0170        | (0.0235) | 9     | 0.0345        | (0.0205) | 14    | 0.0927        | (0.0506) | 4     |
| Cyclopentene_1methyl                                   | C6H10   | 82  | 2 | 67   | 0.0202        | (0.0298) | 9     | 0.0466        | (0.0259) | 13    | 0.1109        | (0.0539) | 4     |
| Hexadiene_cis13  | C6H10   | 82  | 2 | 67   | 0.0026        | (0.0037) | 9     | 0.0044        | (0.0030) | 14    | 0.0097        | (0.0018) | 4     |
| Hexadiene_trans13                                      | C6H10   | 82  | 2 | 67   | 0.0039        | (0.0081) | 9     | 0.0045        | (0.0042) | 12    | 0.0266        | (0.0151) | 4     |
| Other C6H10 (sum of 5 isomers)                         | C6H10   | 82  | 2 | 67   | 0.0348        | (0.0466) | 9     | 0.0531        | (0.0418) | 16    | 0.1954        | (0.0798) | 4     |
| Heptadiyne (sum of 2 isomers)                          | C7H8    | 92  | 4 | 91   | 0.0073        | (0.0094) | 9     | 0.0035        | (0.0053) | 16    | 0.0464        | (0.0394) | 4     |
| Cyclohexene_1methyl                                    | C7H12   | 96  | 2 | 81   | 0.0098        | (0.0120) | 8     | 0.0262        | (0.0139) | 13    | 0.0437        | (0.0259) | 4     |
| Octadiene  | C8H14   | 110 | 2 | 55   | 0.0347        | (0.0531) | 9     | 0.0673        | (0.0416) | 16    | 0.1387        | (0.0536) | 4     |
| Nonadiene  | C9H16   | 124 | 2 | 54   | 0.0020        | (0.0027) | 9     | 0.0048        | (0.0048) | 16    | 0.0171        | (0.0077) | 4     |
| C10H14 non-aromatic (e.g., hexahydronaphthalene)       | C10H14  | 134 | 4 | 91   | 0.0013        | (0.0018) | 9     | 0.0041        | (0.0055) | 16    | 0.0155        | (0.0090) | 4     |
| <b>Terpenes (Polyunsaturated D &gt; 1)</b>             |         |     |   |      |               |          |       |               |          |       |               |          |       |
| Isoprene   | C5H8    | 68  | 2 | 67   | <b>0.1289</b> | (0.1447) | 29    | <b>0.2428</b> | (0.1944) | 23    | <b>0.6942</b> | (0.4405) | 4     |
| Camphene   | C10H16  | 136 | 3 | 93   | 0.0032        | (0.0026) | 9     | 0.0538        | (0.0979) | 14    | 0.1193        | (0.1459) | 4     |
| Carene_3   | C10H16  | 136 | 3 | 93   | 0.0050        | (0.0052) | 8     | 0.0289        | (0.0303) | 12    | 0.1578        | (0.2107) | 4     |
| Limonene_D   | C10H16  | 136 | 3 | 68   | <b>0.0219</b> | (0.0249) | 29    | <b>0.1232</b> | (0.1302) | 23    | <b>0.8384</b> | (1.1869) | 4     |
| Limonene_iso   | C10H16  | 136 | 3 | 68   | 0.0002        | (0.0005) | 9     | 0.0094        | (0.0109) | 16    | 0.0237        | (0.0206) | 4     |
| Myrcene  | C10H16  | 136 | 3 | 93   | 0.0075        | (0.0106) | 8     | 0.0068        | (0.0055) | 10    | 0.1313        | (0.1849) | 4     |
| Pinene_alpha   | C10H16  | 136 | 3 | 93   | 0.0058        | (0.0051) | 9     | <b>0.1013</b> | (0.1454) | 15    | <b>0.8105</b> | (1.2079) | 4     |
| Pinene_beta  | C10H16  | 136 | 3 | 93   | 0.0051        | (0.0092) | 29    | 0.0194        | (0.0220) | 23    | 0.1638        | (0.1545) | 4     |
| Terpinene_gamma  | C10H16  | 136 | 3 | 93   | 0.0044        | (0.0026) | 5     | 0.0118        | (0.0066) | 4     | 0.0310        | (0.0336) | 2     |
| Terpinolene  | C10H16  | 136 | 3 | 93   | 0.0053        | (0.0020) | 4     | 0.0131        | (0.0163) | 8     | 0.0339        | (0.0435) | 4     |
| Sesquiterpenes (sum of all isomers)                    | C15H24  | 204 | 4 | 205+ | <b>0.0092</b> | (0.0088) | 29    | 0.0669        | (0.0786) | 23    | 0.0915        | (0.0659) | 4     |

## Biomass burning emissions and potential air quality impacts

J. B. Gilman et al.

Title Page

Abstract

Introduction

Conclusions

References

Tables

Figures

◀

▶

◀

▶

Back

Close

Full Screen / Esc

Printer-friendly Version

Interactive Discussion



Table 2. Continued.

| Name   | Formula | MW  | D | m/z | SW Avg        | (±SD)    | npnts | SE Avg        | (±SD)    | npnts | N Avg         | (±SD)    | npnts |
|--|---------|-----|---|-----|---------------|----------|-------|---------------|----------|-------|---------------|----------|-------|
| <b>Aromatics with saturated substituents (<math>D = 4</math>)</b>      |         |     |   |     |               |          |       |               |          |       |               |          |       |
| Benzene  | C6H6    | 78  | 4 | 78  | <b>0.8385</b> | (0.7301) | 29    | <b>0.7008</b> | (0.3680) | 23    | <b>2.1381</b> | (1.3236) | 4     |
| Toluene  | C7H8    | 92  | 4 | 91  | <b>0.3549</b> | (0.3417) | 29    | <b>0.6196</b> | (0.4414) | 23    | <b>1.3375</b> | (0.5725) | 4     |
| Benzene_ethyl  | C8H10   | 106 | 4 | 91  | 0.0495        | (0.0498) | 29    | 0.0829        | (0.0583) | 23    | 0.1766        | (0.0919) | 4     |
| Xylene_o   | C8H10   | 106 | 4 | 91  | 0.0391        | (0.0418) | 29    | 0.0730        | (0.0527) | 23    | 0.1429        | (0.0579) | 4     |
| Xylenes_m&p (sum of 2 isomers)   | C8H10   | 106 | 4 | 91  | 0.0981        | (0.1136) | 29    | <b>0.2107</b> | (0.1546) | 23    | <b>0.5088</b> | (0.2484) | 4     |
| Benzene_123trimethyl   | C9H12   | 120 | 4 | 105 | 0.0150        | (0.0137) | 9     | 0.0617        | (0.0425) | 15    | 0.0906        | (0.0562) | 4     |
| Benzene_124trimethyl   | C9H12   | 120 | 4 | 105 | 0.0172        | (0.0217) | 29    | 0.0416        | (0.0291) | 23    | 0.0828        | (0.0339) | 4     |
| Benzene_135trimethyl   | C9H12   | 120 | 4 | 105 | 0.0090        | (0.0083) | 9     | 0.0234        | (0.0154) | 15    | 0.0401        | (0.0158) | 4     |
| Benzene_1ethyl_2methyl   | C9H12   | 120 | 4 | 105 | 0.0094        | (0.0114) | 9     | 0.0164        | (0.0122) | 15    | 0.0374        | (0.0193) | 4     |
| Benzene_1ethyl_3&4_methyl (sum of 2 isomers)                           | C9H12   | 120 | 4 | 105 | 0.0186        | (0.0228) | 29    | 0.0395        | (0.0312) | 23    | 0.1265        | (0.0737) | 4     |
| Benzene_isoPropyl  | C9H12   | 120 | 4 | 105 | 0.0041        | (0.0042) | 9     | 0.0073        | (0.0065) | 14    | 0.0290        | (0.0211) | 4     |
| Benzene_nPropyl  | C9H12   | 120 | 4 | 91  | 0.0081        | (0.0096) | 9     | 0.0173        | (0.0102) | 14    | 0.0331        | (0.0204) | 4     |
| Benzene_isoButyl   | C10H14  | 134 | 4 | 91  | 0.0056        | (0.0065) | 9     | 0.0119        | (0.0104) | 16    | 0.0248        | (0.0145) | 4     |
| Benzene_nButyl   | C10H14  | 134 | 4 | 91  | 0.0065        | (0.0078) | 9     | 0.0151        | (0.0129) | 16    | 0.0329        | (0.0193) | 4     |
| Benzene_1methyl_4isopropyl (p-Cymene)                                  | C10H14  | 134 | 4 | 119 | <b>0.1081</b> | (0.2713) | 29    | 0.1030        | (0.0974) | 23    | 0.1726        | (0.1400) | 4     |
| Benzene_nPropyl_methyl (sum of 2 isomers)                              | C10H14  | 134 | 4 | 105 | 0.0074        | (0.0084) | 9     | 0.0200        | (0.0187) | 16    | 0.0420        | (0.0213) | 4     |
| Benzene_14diethyl  | C10H14  | 134 | 4 | 119 | 0.0007        | (0.0011) | 9     | 0.0018        | (0.0039) | 16    | 0.0165        | (0.0074) | 4     |
| Xylene_ethyl (sum of 2 isomers)  | C10H14  | 134 | 4 | 119 | 0.0093        | (0.0102) | 9     | 0.0149        | (0.0144) | 16    | 0.0379        | (0.0158) | 4     |
| <b>Aromatics with unsaturated substituents (<math>D &gt; 4</math>)</b> |         |     |   |     |               |          |       |               |          |       |               |          |       |
| Benzene_ethynyl (Phenylethyne)   | C8H6    | 102 | 6 | 102 | <b>0.0323</b> | (0.0238) | 9     | 0.0153        | (0.0163) | 16    | 0.0686        | (0.0700) | 4     |
| Styrene (Phenylethene)   | C8H8    | 104 | 5 | 104 | <b>0.0883</b> | (0.0840) | 29    | <b>0.1067</b> | (0.1054) | 23    | <b>0.3361</b> | (0.2437) | 4     |
| Indene   | C9H8    | 116 | 6 | 115 | <b>0.0358</b> | (0.0446) | 9     | <b>0.4008</b> | (0.0325) | 16    | <b>0.1311</b> | (0.1116) | 4     |
| Benzene_1propenyl  | C9H10   | 118 | 5 | 117 | 0.0046        | (0.0054) | 9     | 0.0039        | (0.0045) | 16    | 0.0135        | (0.0074) | 4     |
| Benzene_2propenyl  | C9H10   | 118 | 5 | 117 | 0.0067        | (0.0066) | 9     | 0.0097        | (0.0080) | 16    | 0.0236        | (0.0103) | 4     |
| Benzene_isoPropenyl  | C9H10   | 118 | 5 | 118 | 0.0052        | (0.0059) | 9     | 0.0049        | (0.0050) | 16    | 0.0232        | (0.0129) | 4     |
| Styrene_2methyl  | C9H10   | 118 | 5 | 117 | 0.0142        | (0.0125) | 9     | 0.0153        | (0.0140) | 16    | 0.0414        | (0.0176) | 4     |
| Styrene_3methyl  | C9H10   | 118 | 5 | 117 | 0.0229        | (0.0255) | 9     | <b>0.0297</b> | (0.0234) | 16    | <b>0.0865</b> | (0.0420) | 4     |
| Styrene_4methyl  | C9H10   | 118 | 5 | 117 | 0.0080        | (0.0097) | 9     | 0.0143        | (0.0116) | 16    | 0.0314        | (0.0122) | 4     |
| Indane   | C9H10   | 118 | 5 | 117 | 0.0084        | (0.0066) | 8     | 0.0155        | (0.0069) | 13    | 0.0261        | (0.0108) | 4     |
| Naphthalene  | C10H8   | 128 | 7 | 128 | 0.0070        | (0.0048) | 9     | 0.0040        | (0.0050) | 16    | 0.0215        | (0.0122) | 4     |
| Indene_1or3methyl  | C10H10  | 130 | 6 | 130 | 0.0010        | (0.0009) | 9     | 0.0004        | (0.0011) | 16    | 0.0079        | (0.0059) | 4     |
| Naphthalene_12dihydro  | C10H10  | 130 | 6 | 130 | 0.0062        | (0.0054) | 9     | 0.0099        | (0.0103) | 16    | 0.0277        | (0.0106) | 4     |
| Naphthalene_13dihydro  | C10H10  | 130 | 6 | 130 | 0.0062        | (0.0066) | 9     | 0.0099        | (0.0113) | 16    | 0.0339        | (0.0120) | 4     |
| Benzene_1butenyl   | C10H12  | 132 | 5 | 117 | 0.0021        | (0.0028) | 9     | 0.0027        | (0.0038) | 16    | 0.0140        | (0.0048) | 4     |
| Benzene_methylpropenyl (2-phenyl-2-butene)                             | C10H12  | 132 | 5 | 117 | 0.0274        | (0.0443) | 9     | 0.0179        | (0.0179) | 16    | 0.0436        | (0.0270) | 4     |
| Styrene_ethyl  | C10H12  | 132 | 5 | 117 | 0.0048        | (0.0052) | 9     | 0.0063        | (0.0105) | 16    | 0.0196        | (0.0085) | 4     |

# Biomass burning emissions and potential air quality impacts

J. B. Gilman et al.

Title Page

Abstract

Introduction

Conclusions

References

Tables

Figures

⏪

⏩

⏴

⏵

Back

Close

Full Screen / Esc

Printer-friendly Version

Interactive Discussion

Table 2. Continued.

| Name  | Formula | MW  | D | m/z | SW Avg        | (±SD)    | npnts | SE Avg         | (±SD)    | npnts | N Avg          | (±SD)     | npnts |
|---|---------|-----|---|-----|---------------|----------|-------|----------------|----------|-------|----------------|-----------|-------|
| <b>Nitrogen-containing organics</b>                   |         |     |   |     |               |          |       |                |          |       |                |           |       |
| Acid_Hydrocyanic (Hydrogen cyanide)                   | HCN     | 27  | 2 | IR  | <b>1.2331</b> | (1.2922) | 29    | <b>2.7807</b>  | (1.6904) | 23    | <b>3.0223</b>  | (2.2719)  | 4     |
| Acid_Isocyanic  | HNCO    | 43  | 2 | 42- | <b>0.8433</b> | (0.6858) | 16    | <b>0.8046</b>  | (0.5742) | 17    | <b>1.3360</b>  | (0.2301)  | 2     |
| Methylnitrite (Nitrous acid, methyl ester)            | CH3NO2  | 61  | 1 | 61  | <b>0.8994</b> | (1.1114) | 7     | 0.5241         | (0.5064) | 12    | 0.7641         | (0.8964)  | 3     |
| Nitromethane  | CH3NO2  | 61  | 1 | 61  | 0.0272        | (0.0237) | 9     | 0.0323         | (0.0326) | 16    | 0.0713         | (0.0868)  | 4     |
| Acetonitrile  | C2H3N   | 41  | 2 | 41  | 0.7731        | (0.9389) | 29    | <b>0.9841</b>  | (0.5366) | 23    | <b>1.6524</b>  | (0.8811)  | 4     |
| Hydrazine_11dimethyl                                  | C2H8N2  | 60  | 0 | 60  | 0.0636        | (0.1324) | 9     | 0.1360         | (0.2705) | 16    | 0.1976         | (0.2297)  | 4     |
| Propenenitrile_2 (Acrylonitrile)                      | C3H3N   | 53  | 3 | 53  | 0.0869        | (0.0731) | 29    | 0.1199         | (0.0754) | 23    | 0.3217         | (0.2551)  | 4     |
| Propanenitrile (Cyanoethane)                          | C3H5N   | 55  | 2 | 54  | 0.0314        | (0.0380) | 9     | 0.0432         | (0.0366) | 16    | 0.0981         | (0.0803)  | 4     |
| Pyroline  | C4H5N   | 67  | 3 | 67  | 0.0393        | (0.0591) | 9     | 0.0367         | (0.0392) | 16    | 0.1066         | (0.1088)  | 4     |
| Pyrazole_1methyl                                      | C4H6N2  | 82  | 3 | 82  | 0.0074        | (0.0073) | 9     | 0.0198         | (0.0176) | 16    | 0.0359         | (0.0161)  | 4     |
| Diazine_methyl (sum of 3 isomers)                     | C5H6N2  | 94  | 4 | 94  | 0.0292        | (0.0312) | 9     | 0.0535         | (0.0456) | 16    | 0.1125         | (0.0303)  | 4     |
| Pyrrrole_1methyl                                      | C5H7N   | 81  | 3 | 80  | 0.0202        | (0.0299) | 9     | 0.0083         | (0.0105) | 16    | 0.0217         | (0.0304)  | 4     |
| Pyrazine_2ethyl                                       | C6H8N2  | 108 | 4 | 108 | 0.0062        | (0.0092) | 9     | 0.0152         | (0.0113) | 16    | 0.0296         | (0.0168)  | 4     |
| Benzonitrile (Cyanobenzene)                           | C7H5N   | 103 | 6 | 103 | 0.0622        | (0.0334) | 9     | 0.1395         | (0.0757) | 16    | 0.1380         | (0.0746)  | 4     |
| <b>OVOCs with low degrees of unsaturation (D = 1)</b> |         |     |   |     |               |          |       |                |          |       |                |           |       |
| Formaldehyde  | CH2O    | 30  | 1 | IR  | <b>5.3939</b> | (3.1497) | 29    | <b>12.2348</b> | (7.2935) | 23    | <b>17.9180</b> | (10.5410) | 4     |
| Acid_Formic   | CH2O2   | 46  | 1 | IR  | 0.6359        | (0.5705) | 29    | 1.6007         | (1.1054) | 23    | 1.7538         | (1.9738)  | 4     |
| Methanol  | CH4O    | 32  | 0 | 31  | <b>3.6175</b> | (2.9726) | 29    | <b>7.7807</b>  | (5.5412) | 23    | <b>13.6991</b> | (8.7348)  | 4     |
| Acetaldehyde  | C2H4O   | 44  | 1 | 44  | 1.5503        | (1.1511) | 29    | 2.8332         | (1.8131) | 23    | 5.4742         | (3.5540)  | 4     |
| Acid_Acetic   | C2H4O2  | 60  | 1 | IR  | <b>5.3926</b> | (3.2343) | 29    | <b>13.0293</b> | (8.8369) | 23    | <b>9.6068</b>  | (6.2350)  | 4     |
| Formate_methyl (Formic Acid, methyl ester)            | C2H4O2  | 60  | 1 | 60  | 0.0675        | (0.0390) | 8     | 0.1031         | (0.0626) | 15    | 0.2096         | (0.0831)  | 4     |
| Acid_Glycolic   | C2H4O3  | 76  | 1 | 75- | 0.0068        | (0.0061) | 15    | 0.1183         | (0.1251) | 17    | 0.0114         | (0.0115)  | 2     |
| Ethanol   | C2H6O   | 46  | 0 | 31  | 0.0498        | (0.0617) | 29    | 0.4817         | (0.8472) | 23    | 0.2673         | (0.1892)  | 4     |
| Acetone   | C3H6O   | 58  | 1 | 43  | 0.6501        | (0.7408) | 29    | 1.6035         | (1.1498) | 23    | 2.6208         | (1.0656)  | 4     |
| Propanal  | C3H6O   | 58  | 1 | 58  | 0.2135        | (0.2333) | 29    | 0.4497         | (0.3177) | 23    | 0.9246         | (0.3186)  | 4     |
| Acetate_methyl (Acetic Acid, methyl ester)            | C3H6O2  | 74  | 1 | 74  | 0.4593        | (0.4854) | 9     | 0.6741         | (0.4345) | 16    | 0.6537         | (0.3598)  | 4     |
| Formate_ethyl (Formic Acid, ethyl ester)              | C3H6O2  | 74  | 1 | 30  | 0.0214        | (0.0157) | 5     | 0.0349         | (0.0160) | 10    | 0.0472         | (0.0228)  | 4     |
| Butanal_n   | C4H8O   | 72  | 1 | 72  | 0.0496        | (0.0610) | 29    | 0.0850         | (0.0641) | 23    | 0.1971         | (0.0829)  | 4     |
| Butanone_2 (MEK)                                      | C4H8O   | 72  | 1 | 43  | 0.1788        | (0.2216) | 29    | 0.4143         | (0.3061) | 23    | 0.8027         | (0.3109)  | 4     |
| Propanal_2methyl                                      | C4H8O   | 72  | 1 | 72  | 0.0535        | (0.0599) | 9     | 0.1426         | (0.0933) | 15    | 0.1657         | (0.0976)  | 4     |
| Pyropanoate_methyl (Prop-anoic Acid, methyl ester)    | C4H8O2  | 88  | 1 | 88  | 0.0064        | (0.0085) | 9     | 0.0081         | (0.0082) | 16    | 0.0186         | (0.0110)  | 4     |
| Butanol_1   | C4H10O  | 74  | 0 | 56  | 0.8294        | (1.6678) | 8     | 0.2327         | (0.2540) | 16    | 0.1434         | (0.0695)  | 4     |
| Butanal_2methyl                                       | C5H10O  | 86  | 1 | 57  | 0.0442        | (0.0476) | 9     | 0.1398         | (0.0760) | 13    | 0.1323         | (0.0939)  | 4     |
| Butanone_2_3methyl                                    | C5H10O  | 86  | 1 | 43  | 0.0243        | (0.0315) | 9     | 0.0780         | (0.0394) | 14    | 0.1092         | (0.0551)  | 4     |
| Pentanone_2   | C5H10O  | 86  | 1 | 43  | 0.0576        | (0.0457) | 8     | 0.1095         | (0.0537) | 14    | 0.1791         | (0.0935)  | 4     |
| Pentanone_3   | C5H10O  | 86  | 1 | 57  | 0.0381        | (0.0366) | 8     | 0.0869         | (0.0483) | 15    | 0.1330         | (0.0562)  | 4     |
| Butanoate_methyl (Butyric Acid, methyl ester)         | C5H10O2 | 102 | 1 | 74  | 0.0024        | (0.0041) | 9     | 0.0558         | (0.1431) | 16    | 0.0097         | (0.0063)  | 4     |
| Hexanal_n   | C6H12O  | 100 | 1 | 56  | 0.0192        | (0.0223) | 29    | 0.0342         | (0.0224) | 23    | 0.0635         | (0.0431)  | 4     |
| Hexanone_2  | C6H12O  | 100 | 1 | 43  | 0.0101        | (0.0063) | 8     | 0.0269         | (0.0092) | 12    | 0.0462         | (0.0268)  | 4     |
| Hexanone_3  | C6H12O  | 100 | 1 | 43  | 0.0314        | (0.0315) | 9     | 0.0834         | (0.0317) | 13    | 0.1646         | (0.0868)  | 4     |

Biomass burning  
emissions and  
potential air quality  
impacts

J. B. Gilman et al.

Title Page

Abstract

Introduction

Conclusions

References

Tables

Figures



Back

Close

Full Screen / Esc

Printer-friendly Version

Interactive Discussion

Table 2. Continued.

| Name   | Formula | MW  | D | m/z  | SW Avg        | (±SD)    | npnts | SE Avg        | (±SD)    | npnts | N Avg         | (±SD)    | npnts |
|--|---------|-----|---|------|---------------|----------|-------|---------------|----------|-------|---------------|----------|-------|
| <b>OVOCs with high degrees of unsaturation (<math>D &gt; 1</math>)</b> |         |     |   |      |               |          |       |               |          |       |               |          |       |
| Propenal_2 (Acrolein)  | C3H4O   | 56  | 2 | 56   | <b>0.8189</b> | (0.6824) | 29    | <b>1.3107</b> | (0.8906) | 23    | <b>3.5441</b> | (1.6919) | 4     |
| Acid_Acrylic   | C3H4O2  | 72  | 2 | 71–  | 0.0409        | (0.0438) | 16    | 0.2159        | (0.1637) | 17    | 0.3672        | (0.3881) | 2     |
| Acid_Pyruvic   | C3H4O3  | 88  | 2 | 87–  | 0.0140        | (0.0140) | 15    | 0.1073        | (0.1266) | 17    | 0.0562        | (0.0537) | 2     |
| Butenal_2 (Crotonaldehyde)   | C4H6O   | 70  | 2 | 70   | 0.1218        | (0.1286) | 29    | 0.3234        | (0.2207) | 23    | 0.5275        | (0.1642) | 4     |
| Methacrolein (MACR)  | C4H6O   | 70  | 2 | 41   | 0.0895        | (0.1077) | 29    | 0.1807        | (0.1257) | 23    | 0.5501        | (0.3146) | 4     |
| Methylvinylketone (MVK)  | C4H6O   | 70  | 2 | 55   | 0.4003        | (0.5191) | 29    | 0.8953        | (0.6389) | 23    | 2.1216        | (0.8712) | 4     |
| Butadiene_2,3  | C4H6O2  | 86  | 2 | 86   | 0.2147        | (0.2059) | 29    | 0.6435        | (0.4616) | 23    | 1.2062        | (0.5357) | 4     |
| Acrylate_methyl (2-Propenoic Acid, methyl ester)                       | C4H6O2  | 86  | 2 | 85   | 0.0159        | (0.0178) | 9     | 0.0223        | (0.0149) | 16    | 0.0470        | (0.0227) | 4     |
| Acetate_vinyl (Acetic Acid, vinyl ester)                               | C4H6O2  | 86  | 2 | 86   | 0.0004        | (0.0012) | 9     | 0.0000        | 0.0000   | 16    | 0.0048        | (0.0095) | 4     |
| Dioxin_14_23dihydro  | C4H6O2  | 86  | 2 | 58   | 0.0023        | (0.0044) | 9     | 0.0043        | (0.0059) | 16    | 0.0179        | (0.0162) | 4     |
| Cyclopentenedione  | C5H4O2  | 96  | 4 | 96   | 0.0056        | (0.0080) | 9     | 0.0265        | (0.0337) | 16    | 0.0401        | (0.0326) | 4     |
| Cyclopentenone   | C5H6O   | 82  | 3 | 82   | 0.0825        | (0.1208) | 9     | <b>0.9873</b> | (1.1659) | 16    | 0.9221        | (0.6570) | 4     |
| Pentenone (e.g., Ethyl vinyl ketone)                                   | C5H8O   | 84  | 2 | 84   | 0.2692        | (0.4437) | 9     | 0.8946        | (0.5222) | 16    | 1.4135        | (0.6686) | 4     |
| Pentanone_cyclo  | C5H8O   | 84  | 2 | 84   | 0.1145        | (0.1015) | 9     | 0.3433        | (0.2471) | 16    | 0.7012        | (0.2870) | 4     |
| Butenal_2_2methyl  | C5H8O   | 84  | 2 | 84   | 0.0072        | (0.0064) | 9     | 0.0250        | (0.0210) | 16    | 0.0384        | (0.0136) | 4     |
| Methacrylate_methyl (Methacrylic Acid, methyl ester)                   | C5H8O2  | 100 | 2 | 100  | 0.0306        | (0.0333) | 9     | 0.1055        | (0.0335) | 13    | 0.1287        | (0.0537) | 4     |
| Phenol   | C6H6O   | 94  | 4 | 95+  | <b>0.4262</b> | (0.4242) | 25    | <b>0.7740</b> | (0.6275) | 21    | <b>2.4947</b> | (1.6182) | 4     |
| Benzene_12&13diol (sum of 2 isomers)                                   | C6H6O2  | 110 | 4 | 109– | 0.2438        | (0.1859) | 13    | <b>3.1107</b> | (3.3461) | 17    | <b>3.9631</b> | (1.9126) | 2     |
| Benzaldehyde   | C7H6O   | 106 | 5 | 77   | 0.2212        | (0.1661) | 29    | 0.4717        | (0.3259) | 23    | 0.6995        | (0.2661) | 4     |
| Phenol_methyl (sum of cresol isomers)                                  | C7H8O   | 108 | 4 | 109+ | <b>0.4807</b> | (0.4799) | 25    | 0.7770        | (0.6290) | 21    | 2.0703        | (1.4093) | 4     |
| <b>Furans (heterocyclic OVOCs, <math>D = 1</math>)</b>                 |         |     |   |      |               |          |       |               |          |       |               |          |       |
| Furan  | C4H4O   | 68  | 3 | 68   | <b>0.2680</b> | (0.2474) | 29    | <b>0.7302</b> | (0.4732) | 23    | <b>1.1090</b> | (0.4337) | 4     |
| Furan_2,5dihydro   | C4H6O   | 70  | 2 | 70   | 0.0083        | (0.0126) | 9     | 0.0154        | (0.0438) | 16    | 0.0071        | (0.0141) | 4     |
| Furan_tetrahydro   | C4H8O   | 72  | 1 | 72   | 0.0022        | (0.0027) | 9     | 0.0014        | (0.0027) | 16    | 0.0101        | (0.0067) | 4     |
| Furaldehyde_2 (Furfural)   | C5H4O2  | 96  | 4 | 95   | <b>0.3567</b> | (0.2119) | 9     | <b>1.5298</b> | (1.0837) | 16    | <b>1.2999</b> | (0.6550) | 4     |
| Furaldehyde_3  | C5H4O2  | 96  | 4 | 95   | 0.0152        | (0.0135) | 9     | 0.0585        | (0.0403) | 16    | 0.0687        | (0.0330) | 4     |
| Furan_2methyl  | C5H6O   | 82  | 3 | 82   | <b>0.2847</b> | (0.3634) | 9     | <b>0.6908</b> | (0.4118) | 16    | <b>1.2105</b> | (0.4806) | 4     |
| Furan_3methyl  | C5H6O   | 82  | 3 | 82   | 0.0272        | (0.0311) | 29    | 0.0776        | (0.0582) | 23    | 0.1708        | (0.0661) | 4     |
| Furan_2,5dimethyl  | C6H8O   | 96  | 3 | 96   | 0.0328        | (0.0472) | 9     | 0.0857        | (0.0587) | 16    | 0.1808        | (0.1005) | 4     |
| Furan_2ethyl   | C6H8O   | 96  | 3 | 81   | 0.0167        | (0.0218) | 29    | 0.0387        | (0.0285) | 23    | 0.0821        | (0.0288) | 4     |
| Benzofuran   | C8H6O   | 118 | 6 | 118  | 0.0902        | (0.0666) | 9     | 0.1366        | (0.0734) | 16    | 0.2504        | (0.0957) | 4     |
| Benzofuran_methyl (sum of 4 isomers)                                   | C9H8O   | 132 | 6 | 131  | 0.0599        | (0.0444) | 9     | 0.1078        | (0.0938) | 16    | 0.1980        | (0.0363) | 4     |

## Biomass burning emissions and potential air quality impacts

J. B. Gilman et al.

Title Page

Abstract

Introduction

Conclusions

References

Tables

Figures

◀

▶

◀

▶

Back

Close

Full Screen / Esc

Printer-friendly Version

Interactive Discussion



Table 2. Continued.

| Name   | Formula                       | MW | D | m/z | SW Avg        | (±SD)        | npnts        | SE Avg        | (±SD)        | npnts        | N Avg         | (±SD)        | npnts        |
|--|-------------------------------|----|---|-----|---------------|--------------|--------------|---------------|--------------|--------------|---------------|--------------|--------------|
| <b>Methane and Inorganic Gases</b>                                       |                               |    |   |     |               |              |              |               |              |              |               |              |              |
| Methane  | CH <sub>4</sub>               | 16 | - | IR  | <b>40.911</b> | (24.945)     | 29           | <b>62.302</b> | (32.218)     | 23           | <b>96.707</b> | (28.737)     | 4            |
| Carbon Monoxide  | CO                            | 28 | - | IR  | <b>1000</b>   | (0)          | 29           | <b>1000</b>   | (0)          | 23           | <b>1000</b>   | (0)          | 4            |
| Carbon Dioxide   | CO <sub>2</sub>               | 44 | - | IR  | <b>18202</b>  | (20970)      | 29           | <b>31170</b>  | (71256)      | 23           | <b>17999</b>  | (14000)      | 4            |
| Tricarbon Dioxide (Carbon suboxide)                                      | C <sub>3</sub> O <sub>2</sub> | 68 | - | 68  | 0.0024        | (0.0030)     | 9            | 0.0040        | (0.0055)     | 16           | 0.0044        | (0.0042)     | 4            |
| Ammonia  | NH <sub>3</sub>               | 17 | - | IR  | 12.530        | (8.838)      | 29           | 14.797        | (6.131)      | 23           | 20.761        | (16.928)     | 4            |
| Nitrogen Oxide   | NO                            | 30 | - | IR  | <b>38.788</b> | (51.194)     | 29           | <b>39.695</b> | (91.842)     | 23           | <b>26.530</b> | (24.243)     | 4            |
| Nitrogen Dioxide   | NO <sub>2</sub>               | 46 | - | IR  | 7.051         | (8.565)      | 29           | 12.254        | (21.246)     | 23           | 10.583        | (10.218)     | 4            |
| Nitrous Acid   | HONO                          | 47 | - | 46- | 2.504         | (2.827)      | 16           | 4.563         | (6.049)      | 17           | 4.946         | (5.254)      | 2            |
| Sulfur Dioxide   | SO <sub>2</sub>               | 64 | - | IR  | 5.600         | (9.993)      | 29           | 7.901         | (14.488)     | 23           | 8.408         | (5.347)      | 4            |
| Hydrochloric Acid  | HCl                           | 36 | - | IR  | 0.992         | (2.574)      | 29           | 1.398         | (4.825)      | 23           | 0.472         | (0.719)      | 4            |
| <b>Total ERs (mmol (mol CO)<sup>-1</sup>)</b>                            |                               |    |   |     | <b>19356</b>  |              |              | <b>32403</b>  |              |              | <b>19317</b>  |              |              |
| Σ ERs for all nitrogen-containing species (mmol (mol CO) <sup>-1</sup> ) |                               |    |   |     | <b>65</b>     | <b>0.34%</b> | <b>N</b>     | <b>77</b>     | <b>0.24%</b> | <b>N</b>     | <b>71</b>     | <b>0.37%</b> | <b>N</b>     |
| Σ ERs for all VOCs and % of total emissions                              |                               |    |   |     | <b>46</b>     | <b>0.24%</b> | <b>VOC</b>   | <b>90</b>     | <b>0.28%</b> | <b>VOC</b>   | <b>150</b>    | <b>0.78%</b> | <b>VOC</b>   |
| Σ ERs for unsaturated VOCs and % of total VOC                            |                               |    |   |     | <b>39</b>     | <b>84%</b>   | <b>Unsat</b> | <b>74</b>     | <b>82%</b>   | <b>Unsat</b> | <b>126</b>    | <b>84%</b>   | <b>Unsat</b> |
| Σ ERs for oxygenated VOCs and % of total VOC                             |                               |    |   |     | <b>24</b>     | <b>53%</b>   | <b>Oxy</b>   | <b>57</b>     | <b>63%</b>   | <b>Oxy</b>   | <b>81</b>     | <b>54%</b>   | <b>Oxy</b>   |

MW = molecular weight (g mol<sup>-1</sup>); D = Degrees of unsaturation; m/z = mass fragment used to quantify a species where (+) denotes measurements by the PTR-MS or PIT-MS, (-) denotes measurements by the NI-PT-GIMS, and (IR) denotes measurements by the OP-FTIR. All other measurements are by GC-MS; avg = mean; SD = standard deviation; and npnts = number of points used to calculate average and standard deviation.

**Bold ER** = largest 3 ERs for each compound class.

**Bold and italic ER** = largest 3 ERs for all VOCs.

Description of naming scheme: propane\_22dimethyl is equivalent to 2,2-dimethylpropane. If the exact compound identity could not be determined, then the species are identified using general names that reflect the chemical family and formula are used. For example, hexenes (sum of 3 isomers) may include species such as cis- and trans-3-hexene. Alternative names, such as p-Cymene for 1-methyl-4-isopropylbenzene, or common abbreviations such as MEK for Butanone\_2 are also included.

## Biomass burning emissions and potential air quality impacts

J. B. Gilman et al.

Title Page

Abstract

Introduction

Conclusions

References

Tables

Figures

⏪

⏩

◀

▶

Back

Close

Full Screen / Esc

Printer-friendly Version

Interactive Discussion



**Table 3.** Slopes and correlation coefficients ( $r$ ) for VOC to carbon monoxide (CO) and VOC to acetonitrile ( $\text{CH}_3\text{CN}$ ) ratios observed in biomass burning (BB) plumes from the Fourmile Canyon Fire as identified in Fig. 6.

| VOC Name              | VOC vs. CO |      | VOC vs. $\text{CH}_3\text{CN}$ |      | Emission Sources |       |          | Rxn Rate Coefficient |                              |
|-----------------------|------------|------|--------------------------------|------|------------------|-------|----------|----------------------|------------------------------|
|                       | Slope      | $r$  | Slope                          | $r$  | BB               | Urban | Biogenic | $k\text{OH}^a$       | vs. $\text{CH}_3\text{CN}^b$ |
| <b>Furan_2methyl</b>  | 0.0003     | 0.88 | 0.0470                         | 0.95 | yes              |       |          | 111                  | 5550                         |
| Carene_3              | 0.0004     | 0.96 | 0.0654                         | 0.98 | yes              |       | yes      | 85                   | 4250                         |
| <b>Furan</b>          | 0.0004     | 0.70 | 0.1153                         | 0.95 | yes              |       |          | 67                   | 3355                         |
| Butadiene_13          | 0.0002     | 0.98 | 0.0296                         | 0.94 | yes              | yes   |          | 67                   | 3330                         |
| Styrene               | 0.0001     | 0.97 | 0.0209                         | 0.94 | yes              | yes   | yes      | 58                   | 2900                         |
| Propene_2methyl       | 0.0004     | 0.98 | 0.0648                         | 0.98 | yes              | yes   |          | 51                   | 2570                         |
| <b>Furaldehyde_2</b>  | 0.0003     | 0.93 | 0.0491                         | 0.98 | yes              |       |          | 48                   | 2400                         |
| <b>Benzofuran</b>     | 0.0001     | 0.97 | 0.0210                         | 0.99 | yes              |       |          | 37                   | 1860                         |
| Butene_1              | 0.0004     | 0.98 | 0.0571                         | 0.99 | yes              | yes   |          | 31                   | 1570                         |
| Propene               | 0.0040     | 0.97 | 0.6385                         | 0.99 | yes              | yes   |          | 26                   | 1315                         |
| Propanal              | 0.0010     | 0.95 | 0.1481                         | 0.90 | yes              | yes   |          | 20                   | 1000                         |
| Propenal_2            | 0.0009     | 0.98 | 0.1366                         | 0.98 | yes              | yes   |          | 19                   | 955                          |
| p-Cymene <sup>c</sup> | 0.0003     | 0.97 | 0.0415                         | 0.97 | yes              |       | yes      | 15                   | 750                          |
| Benzaldehyde          | 0.0010     | 0.98 | 0.1444                         | 0.95 | yes              |       | yes      | 14                   | 700                          |
| Ethene                | 0.0082     | 0.97 | 1.3526                         | 0.92 | yes              | yes   |          | 8.5                  | 425                          |
| Benzene               | 0.0019     | 0.99 | 0.2835                         | 0.96 | yes              | yes   |          | 1.2                  | 60                           |
| Butanone_2 (MEK)      | 0.0010     | 0.93 | 0.1640                         | 0.94 | yes              | yes   | yes      | 1.2                  | 60                           |
| <b>Benzonitrile</b>   | 0.0003     | 0.88 | 0.0499                         | 0.94 | yes              |       |          | 1.0                  | 50                           |
| Butadione_23          | 0.0002     | 0.77 | 0.0384                         | 0.89 | yes              |       | yes      | 0.25                 | 12.5                         |
| <b>Acetonitrile</b>   | 0.0062     | 0.96 | 1.0000                         | 1.00 | yes              |       |          | 0.020                | 1                            |

**Bold** face denotes VOCs that are the best available BB markers.

<sup>a</sup> Rxn Rate Coefficient  $\times 10^{12}$  = first order reaction rate coefficient of VOC + OH reaction at STP.

<sup>b</sup> Ratio of rxn rate coefficients for VOC vs. acetonitrile ( $\text{CH}_3\text{CN}$ )  $\times 10^{12}$  at STP.

<sup>c</sup> Benzene\_1methyl\_4isopropyl.

## Biomass burning emissions and potential air quality impacts

J. B. Gilman et al.

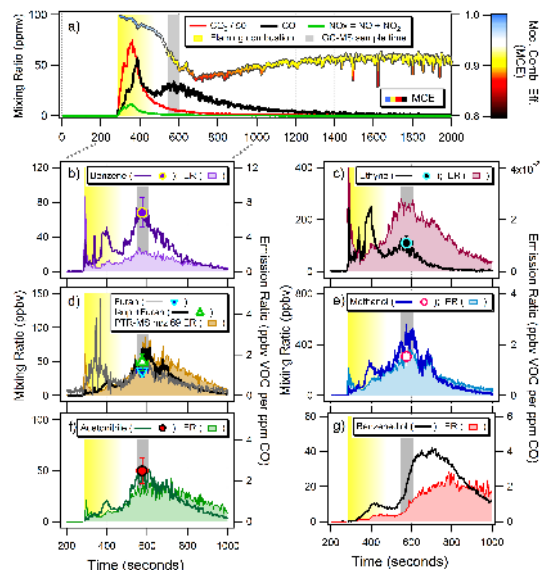


**Figure 1.** Temporal profiles of mixing ratios and emission ratios (ER) of select gases and the modified combustion efficiency (MCE) for an example laboratory burn of Emory Oak Woodland fuel from Fort Huachuca, Arizona. **(a)** Mixing ratios of  $\text{CO}_2$ ,  $\text{CO}$ , and  $\text{NO}_x$  measured by OP-FTIR. The MCE trace is colored by the key and scale on the right. The vertical bars represent the flaming combustion phase of the laboratory burn (yellow) and the GC-MS sample acquisition time (grey). **(b–f)** Discrete GC-MS measured mixing ratios are shown as markers. **(b–g)** Mixing ratios measured by PTR-MS (benzene,  $m/z$  69 = isoprene + furan + other, and acetonitrile), OP-FTIR (furan, ethyne, and methanol), and NI-PT-CIMS (benzenediol) are shown as lines and the corresponding VOC to CO ERs are shown as filled traces.

Title Page

Abstract

Introduction

Conclusions

References

Tables

Figures

◀

▶

◀

▶

Back

Close

Full Screen / Esc

Printer-friendly Version

Interactive Discussion

## Biomass burning emissions and potential air quality impacts

J. B. Gilman et al.

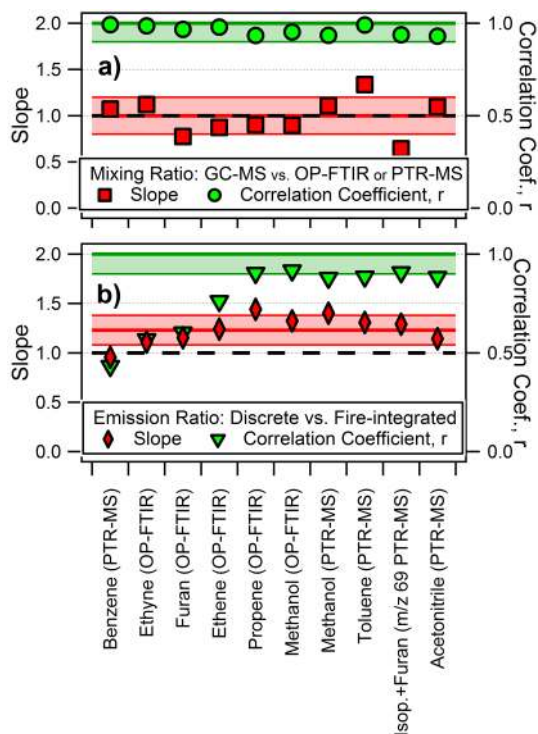


**Figure 2.** Slopes and correlation coefficients,  $r$ , determined from correlation plots of **(a)** mixing ratios measured by the GC-MS vs. the average mixing ratio measured by the OP-FTIR or PTR-MS during the GC-MS sample acquisition time and **(b)** discrete vs. fire-integrated emission ratios of select VOCs relative to CO as measured by the OP-FTIR or PTR-MS. The black dashed line represents slopes equal to 1. The average of the slopes and the standard deviation is shown by the red shaded bands. The green bands represent  $r > 0.90$ .



## Biomass burning emissions and potential air quality impacts

J. B. Gilman et al.

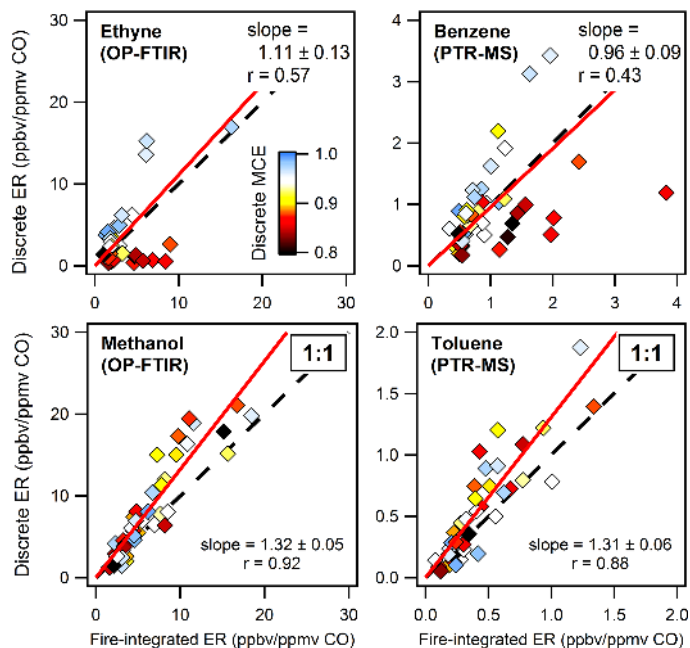


**Figure 3.** Correlation plots of the discrete vs. fire-integrated emission ratios (ER) for ethyne and methanol measured by the OP-FTIR and benzene and toluene measured by the PTR-MS. Each data point represents one biomass burn and are colored by the modified combustion efficiency (MCE) corresponding to the discrete sampling times of the GC-MS. MCE values near unity are associated with flaming combustion and lower MCE values are associated with smoldering combustion. The linear 2-sided regression lines forced through the origin are shown as red lines and the 1 : 1 ratio is shown by the dashed lines.

Title Page

Abstract

Introduction

Conclusions

References

Tables

Figures

◀

▶

◀

▶

Back

Close

Full Screen / Esc

Printer-friendly Version

Interactive Discussion



## Biomass burning emissions and potential air quality impacts

J. B. Gilman et al.

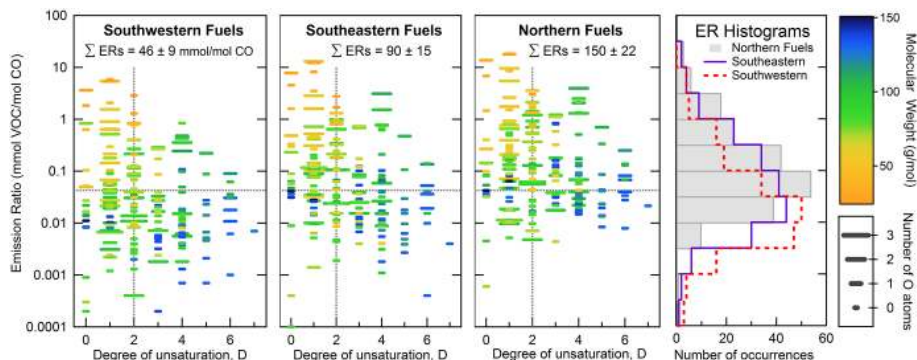


**Figure 4.** Discrete molar emission ratios for all VOCs reported in Table 2 as a function of the degree of unsaturation,  $D$ , for each fuel region. Emission ratios are colored by the corresponding molecular weight and the marker width represents the corresponding number of oxygen (O) atoms. The dashed lines represent the median values for all VOCs from all fuel regions ( $ER = 0.0427 \text{ mmol mol}^{-1} \text{ CO}$  and  $D = 2$ ). The histogram on the right summarizes the distribution of molar emission ratios for each fuel region.

Title Page

Abstract

Introduction

Conclusions

References

Tables

Figures

◀

▶

◀

▶

Back

Close

Full Screen / Esc

Printer-friendly Version

Interactive Discussion



**Biomass burning emissions and potential air quality impacts**

J. B. Gilman et al.

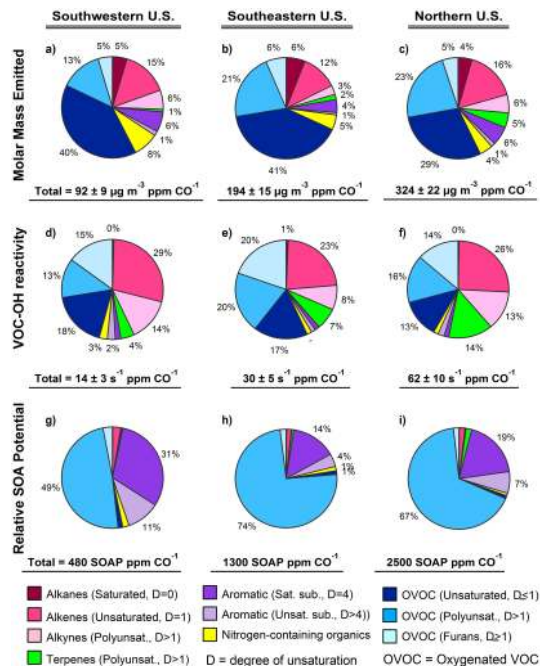


**Figure 5.** Contributions of (non-methane) VOCs reported in Table 2 to (a–c) the molar mass emitted, (d–f) OH reactivity, and (g–i) relative SOA potential for the southwestern, southeastern, and northern fuel regions. Totals for each fuel region are shown below each pie chart.



Title Page

Abstract Introduction

Conclusions References

Tables Figures

◀ ▶

◀ ▶

Back Close

Full Screen / Esc

Printer-friendly Version

Interactive Discussion

## Biomass burning emissions and potential air quality impacts

J. B. Gilman et al.

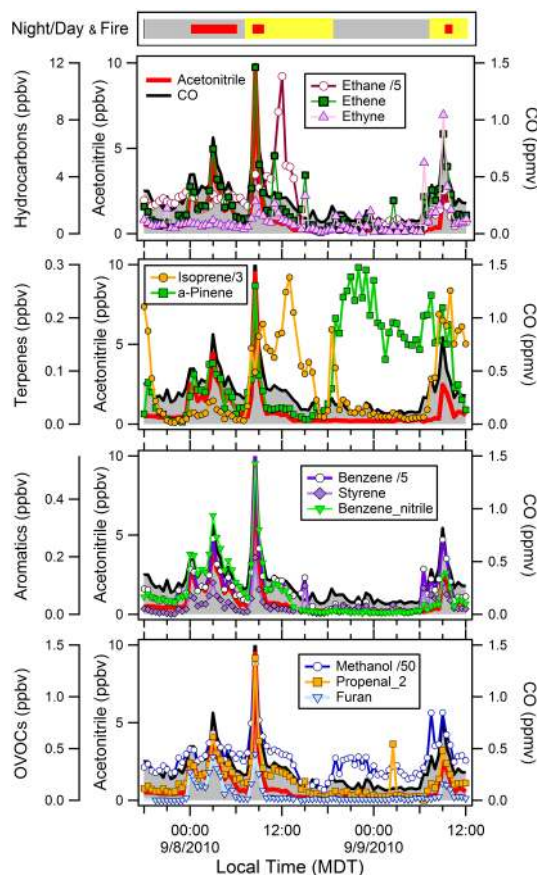


**Figure 6.** Time series of ambient air measurements in Boulder, Colorado, during the Fourmile Canyon Fire. The top bar indicates nighttime (grey), daytime (yellow), and biomass burning plumes (red markers). CO and acetonitrile are included in all 4 panels.

Title Page

Abstract

Introduction

Conclusions

References

Tables

Figures



Back

Close

Full Screen / Esc

Printer-friendly Version

Interactive Discussion



## Biomass burning emissions and potential air quality impacts

J. B. Gilman et al.

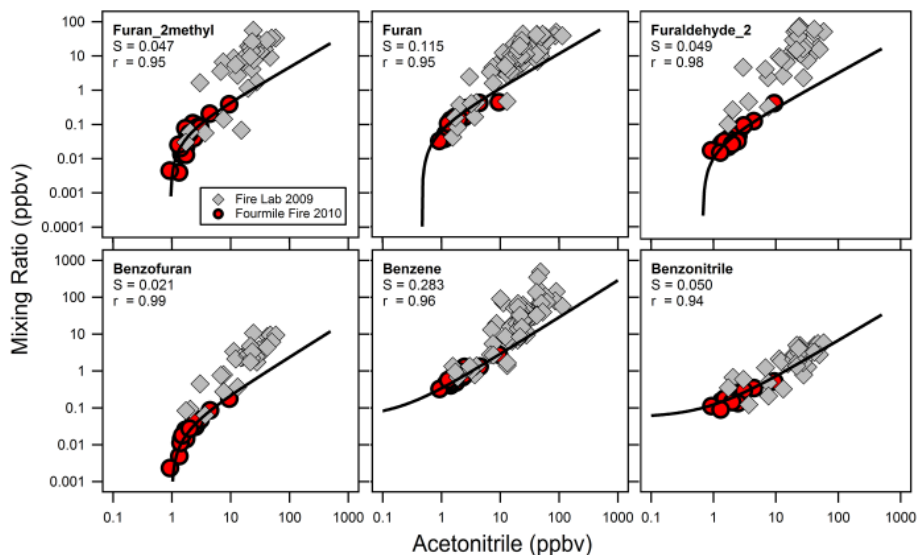


**Figure 7.** Correlation plots of VOCs vs. acetonitrile for all 56 laboratory biomass burns (grey markers) and Fourmile Canyon Fire (red markers correspond to the BB plume identified in Fig. 6).

[Title Page](#)[Abstract](#)[Introduction](#)[Conclusions](#)[References](#)[Tables](#)[Figures](#)[◀](#)[▶](#)[◀](#)[▶](#)[Back](#)[Close](#)[Full Screen / Esc](#)[Printer-friendly Version](#)[Interactive Discussion](#)